



UNIVERSIDAD DE INVESTIGACIÓN DE TECNOLOGÍA EXPERIMENTAL YACHAY

Escuela de Ciencias de la Tierra, Energía y Ambiente

TÍTULO: PETROGRAPHIC AND CHEMICAL ANALYSIS OF MIOCENE DETRITAL HEAVY MINERALS FROM COMALCALCO AND MACUSPANA BASINS, SOUTHEAST OF MEXICO

Trabajo de integración curricular presentado como requisito para la
obtención del título de Geóloga

Autora:

Eva Carolina Andrade Barahona

Tutor:

PhD Germán Martín

Co-tutor:

PhD Theofilos Toulkeridis

Urququí, marzo de 2020

Urcuquí, 5 de marzo de 2020

SECRETARÍA GENERAL
(Vicerrectorado Académico/Cancillería)
ESCUELA DE CIENCIAS DE LA TIERRA, ENERGÍA Y AMBIENTE
CARRERA DE GEOLOGÍA
ACTA DE DEFENSA No. UITEY-GEO-2020-00003-AD

En la ciudad de San Miguel de Urcuquí, Provincia de Imbabura, a los 5 días del mes de marzo de 2020, a las 14:00 horas, en el Aula CHA-01 de la Universidad de Investigación de Tecnología Experimental Yachay y ante el Tribunal Calificador, integrado por los docentes:

Presidente Tribunal de Defensa	Dr. TORO ALAVA, JORGE EDUARDO , Ph.D.
Miembro No Tutor	Dr. SOLTANI DEHNAVI, AZAM , Ph.D.
Tutor	Dr. MARTIN MERINO, GERMAN , Ph.D.

Se presenta el(la) señor(ita) estudiante **ANDRADE BARAHONA, EVA CAROLINA**, con cédula de identidad No. **0302582481**, de la **ESCUELA DE CIENCIAS DE LA TIERRA, ENERGÍA Y AMBIENTE**, de la Carrera de **GEOLOGÍA**, aprobada por el Consejo de Educación Superior (CES), mediante Resolución **RPC-SE-10-No.031-2016**, con el objeto de rendir la sustentación de su trabajo de titulación denominado: **PETROGRAPHIC AND CHEMICAL ANALYSIS OF MIOCENE DETRITAL HEAVY MINERALS FROM COMALCALCO AND MACUSPANA BASINS, SOUTHEAST OF MEXICO**, previa a la obtención del título de **GEÓLOGO/A**.

El citado trabajo de titulación, fue debidamente aprobado por el(los) docente(s):

Tutor	Dr. MARTIN MERINO, GERMAN , Ph.D.
--------------	-----------------------------------

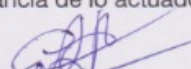
Y recibió las observaciones de los otros miembros del Tribunal Calificador, las mismas que han sido incorporadas por el(la) estudiante.

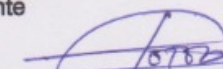
Previamente cumplidos los requisitos legales y reglamentarios, el trabajo de titulación fue sustentado por el(la) estudiante y examinado por los miembros del Tribunal Calificador. Escuchada la sustentación del trabajo de titulación, que integró la exposición de el(la) estudiante sobre el contenido de la misma y las preguntas formuladas por los miembros del Tribunal, se califica la sustentación del trabajo de titulación con las siguientes calificaciones:

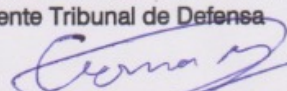
Tipo	Docente	Calificación
Tutor	Dr. MARTIN MERINO, GERMAN , Ph.D.	9,6
Presidente Tribunal De Defensa	Dr. TORO ALAVA, JORGE EDUARDO , Ph.D.	8,8
Miembro Tribunal De Defensa	Dr. SOLTANI DEHNAVI, AZAM , Ph.D.	9,0

Lo que da un promedio de: **9.1 (Nueve punto Uno)**, sobre 10 (diez), equivalente a: **APROBADO**

Para constancia de lo actuado, firman los miembros del Tribunal Calificador, el/la estudiante y el/la secretario ad-hoc.


ANDRADE BARAHONA, EVA CAROLINA
Estudiante


Dr. TORO ALAVA, JORGE EDUARDO , Ph.D.
Presidente Tribunal de Defensa


Dr. MARTIN MERINO, GERMAN , Ph.D.
Tutor

A. Soltani

Dr. SOLTANI DEHNAVI, AZAM , Ph.D.

Miembro No Tutor

[Signature]

TERÁN ROSALES, ANDREA YOLANDA

Secretario Ad-hoc

SECRETARÍA GENERAL
Escuela de Ciencias de la Tierra, Energía y Ambiente
Carrera de Geología
ACTA DE DEFENSA No. UTEY-GEO-2020-0000-AB

En la ciudad de San Miguel de Utcupe, Provincia de Imbabura, a los 5 días del mes de marzo de 2020
en la Aula CHA-01 de la Universidad de Investigación de Tecnología Experimental Yachay y ante el Tribunal Calificador
integrado por los docentes:

de presenta el(los) estudiante(s) ANDRADE BARAHONA, EVA CAROLINA, con cédula de identidad No. 992522981,
de la ESCUELA DE CIENCIAS DE LA TIERRA, ENERGÍA Y AMBIENTE, de la Carrera de GEOLOGÍA, aprobada por el
Consejo de Educación Superior (CES), mediante Resolución RPC-SE-10-NO-081-2018, con el objeto de tener la
sustentación de su trabajo de titulación denominado: PETROGRAPHIC AND CHEMICAL ANALYSIS OF MIOCENE
DETITAL HEAVY MINERALS FROM COMALCALCO AND MACUSPANA BASINS, SOUTHEAST OF MEXICO. Previa a la
opción del título de GEOLOGÍA.

El citado trabajo de titulación, fue debidamente aprobado por el(los) docente(s):

Y recibió las observaciones de los otros miembros del Tribunal Calificador, las mismas que han sido incorporadas por el(los)
estudiante(s).

Previamente cumplidos los requisitos legales y reglamentarios, el trabajo de titulación fue sustentado por el(los) estudiante(s) y
examinado por los miembros del Tribunal Calificador. Escuchada la sustentación del trabajo de titulación, que integro la
exposición de el(los) estudiante(s) sobre el contenido de la misma y las preguntas formuladas por los miembros del Tribunal, se
calificó la sustentación del trabajo de titulación con las siguientes calificaciones:

Tipo	Docente	Calificación
Tutor	Dr. MARTIN MERINO GERMAN, Ph.D.	9.8
Presidente Tribunal de Defensa	Dr. TORO ALAVA, JORGE EDUARDO, Ph.D.	9.8
Miembro Tribunal de Defensa	Dr. SOLTANI DEHNAVI, AZAM, Ph.D.	9.0

Lo que da un promedio de: 9.7 (Nueve punto Uno), sobre 10 (diez), equivalente a: APROBADO

Para constancia de lo actuado, firman los miembros del Tribunal Calificador, el(los) estudiante(s) y el(los) secretario(s) ad-hoc.

[Signature]
ANDRADE BARAHONA, EVA CAROLINA
Estudiante

[Signature]
Dr. TORO ALAVA, JORGE EDUARDO, Ph.D.
Presidente Tribunal de Defensa

[Signature]
Dr. MARTIN MERINO GERMAN, Ph.D.
Tutor

AUTORÍA

Yo, **Eva Carolina Andrade Barahona**, con cédula de identidad 0302582481, declaro que las ideas, juicios, valoraciones, interpretaciones, consultas bibliográficas, definiciones y conceptualizaciones expuestas en el presente trabajo; así como, los procedimientos y herramientas utilizadas en la investigación, son de absoluta responsabilidad de el/la autora (a) del trabajo de integración curricular. Así mismo, me acojo a los reglamentos internos de la Universidad de Investigación de Tecnología Experimental Yachay.

Urcuquí, marzo de 2020.



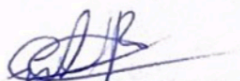
Eva Carolina Andrade Barahona
CI: 0302582481

AUTORIZACIÓN DE PUBLICACIÓN

Yo, **Eva Carolina Andrade Barahona**, con cédula de identidad 0302582481, cedo a la Universidad de Investigación de Tecnología Experimental Yachay, los derechos de publicación de la presente obra, sin que deba haber un reconocimiento económico por este concepto. Declaro además que el texto del presente trabajo de titulación no podrá ser cedido a ninguna empresa editorial para su publicación u otros fines, sin contar previamente con la autorización escrita de la Universidad.

Asimismo, autorizo a la Universidad que realice la digitalización y publicación de este trabajo de integración curricular en el repositorio virtual, de conformidad a lo dispuesto en el Art. 144 de la Ley Orgánica de Educación Superior

Urququí, marzo de 2020.



Eva Carolina Andrade Barahona
CI: 0302582481

DEDICATION

I dedicate this work to my family, who supported me during my university career, especially to my father Patricio Andrade and my mother Eulalia Barahona for their trust during my study time at Yachay Tech; thanks to them I was able to finish my university career.

ACKNOWLEDGEMENTS

I want to thank my advisor Germán Martin for his support and help to fulfill my bachelor thesis project. Thanks to my co-advisor, Theofilos Toulkeridis, for his assistance to accomplish the chemical analysis.

I am thankful to Uwe Martens, who suggested the topic of this project and guided me through the petrographic studies as well as chemical analysis procedure. Furthermore, Uwe was the teacher who inspired me and directed my geology interest into the field of mineralogical and petrographic research. Thanks to María Isabel Sierra, who bring me the samples for my thesis as well as extensive knowledge share.

ABSTRACT

Presented here is a provenance investigation of the oil and gas reservoir basins of southeast Mexico, focusing on heavy detrital minerals of the Miocene sediments deposited in the Comalcalco and Macuspana basins. Based on petrographic analysis of the samples taken from Comalcalco and Macuspana basins, twelve different heavy minerals were identified. These minerals are amphibole, apatite, chloritoid, chlorite, chromian spinel, epidote, garnet, ilmenite, rutile, staurolite, titanite, and zircon. Microanalysis on the heavy mineral of interest carried on using scanning electron microscope (SEM). Among the identified heavy minerals, amphibole, chromian spinel, garnet, and ilmenite are used for the final interpretation. Garnet grains are chemically classified into four different groups, including G1: those grains with 0% of spessartine and high pyrope and almandine content; G2: grains with less than 10% of spessartine and high pyrope and almandine content; G3: grains with 24-39% of spessartine, variable amount of almandine; and G4: grains with more than 70% of spessartine and with almost the same almandine and pyrope content. Various chemical composition of garnet suggests the probably variability in their origin such as Chiapas Massif, Grenvillian Oaxaca, and Guichicovi complexes. Ilmenite occurs in high proportion in almost all samples. Ilmenite can be originated from the ilmenitites found in the Chiapas Massif Complex, and/or the ilmenite-magnetite-apatite and apatite-ilmenite-rich gneisses of the Grenvillian Oaxacan Complex. Additionally, ilmenite can be sourced from the granulites of mafic composition of the Guichicovi Complex. Ti-rich amphibole is another prominent heavy mineral that is likely sourced by the felsic orthogneisses from the Guichicovi Complex. Also, chromian spinel could be derived from the amphibolites of the Chiapas Massif Complex.

KEY WORDS:

Chiapas Massif Complex, Comalcalco basin, chromian spinel, garnet, Guichicovi Complex, heavy minerals, Macuspana basin, Oaxacan Complex, sediment provenance, Southeast of Mexico, Ti-rich amphibole.

RESUMEN

Se presenta una investigación de procedencia de las cuencas de los yacimientos de petróleo y gas del sureste de México, que se centra en los minerales detríticos pesados de los sedimentos del Mioceno depositados en las cuencas de Comalcalco y Macuspana. Mediante un análisis petrográfico de los granos de muestras tomadas de las cuencas de Comalcalco y Macuspana, se determinó la presencia de doce minerales pesados diferentes. Estos minerales son anfíbol, apatito, cloritoide, clorita, espinela cromífera, epidota, granate, ilmenita, rutilo, estaurolita, titanita, y circón. Se llevó a cabo un microanálisis sobre los minerales pesados de interés utilizando un microscopio electrónico de barrido (SEM). Entre los minerales pesados identificados, anfíbol, espinela cromífera, granate, e ilmenita se utilizan para la interpretación final. Los granos de granate se clasificaron en base a su composición química en cuatro grupos diferentes, incluido G1: los granos con 0% de espesartina y alto contenido de piropo y almandina; G2: granos con menos del 10% de espesartina y alto contenido de piropo y almandina; G3: granos con 24-39% de espesartina, cantidad variable de almandina; y G4: granos con más del 70% de espesartina y con casi el mismo contenido de almandina y piropo. La diferente composición química de los granos de granate sugiere la probable variabilidad en su origen, como los complejos Macizo de Chiapas, Oaxaca Grenvilliano y Guichicovi. La ilmenita se presenta en alta proporción en casi todas las muestras. Este mineral pudo originarse a partir de las ilmenitas del Complejo del Macizo de Chiapas, y/o de los gneis ricos en apatito-ilmenita y apatito-ilmenita del Complejo Oaxaca Grenvilliano. Además, la ilmenita puede provenir de granulitas de composición máfica del complejo Guichicovi. El anfíbol rico en Ti es otro mineral pesado representativo que probablemente proviene de los ortogneises félsicos del Complejo Guichicovi. Por otro lado, la espinela cromífera podría derivarse de las anfíbolitas del Complejo Macizo de Chiapas.

PALABRAS CLAVE:

Anfíbol rico en Ti, Complejo de Oaxaca Grenvilliano, Complejo del Macizo de Chiapas, Complejo Guichicovi, cuenca de Macuspana, cuenca de Comalcalco, espinela cromífera, granate, minerales pesados, procedencia de sedimentos, Sureste de México.

LIST OF CONTENTS

1. INTRODUCTION	1
STUDY AREA.....	1
SEDIMENTARY PROVENANCE ANALYSIS	1
PROBLEM STATEMENT	3
OBJECTIVE.....	4
2. DETRITAL HEAVY MINERALS	5
3. GEOLOGICAL FRAMEWORK.....	9
TECTONISM OF THE STUDY AREA.....	10
METAMORPHIC COMPLEXES OF SOUTHEAST OF MEXICO.....	10
CHIAPAS MASSIF COMPLEX (CMC).....	11
GRENVILLIAN COMPLEXES	13
<i>Grenvillian Oaxacan Complex.....</i>	<i>13</i>
<i>Guichicovi Complex.....</i>	<i>14</i>
MACUSPANA AND COMALCALCO BASINS	17
3. LOCATION OF THE STUDY AREA.....	22
SAMPLING LOCATION	22
4. METHODOLOGY	26
SAMPLE PREPARATION	26
SEM ANALYSIS	28
5. RESULTS	30
PETROGRAPHIC RESULTS	30
SEM-EDS RESULTS.....	37
<i>Ti-bearing amphibole</i>	<i>37</i>
<i>Apatite</i>	<i>38</i>
<i>Chlorite</i>	<i>39</i>
<i>Chloritoid</i>	<i>39</i>
<i>Chromian spinel</i>	<i>40</i>
<i>Epidote</i>	<i>41</i>
<i>Garnet</i>	<i>41</i>
<i>Ilmenite</i>	<i>42</i>
<i>Rutile</i>	<i>43</i>
<i>Staurolite.....</i>	<i>44</i>
<i>Titanite</i>	<i>44</i>
<i>Zircon.....</i>	<i>45</i>
6. DISCUSSION	48
7. CONCLUSIONS.....	55
8. REFERENCES	57
10. APPENDIX.....	67
APPENDIX 1.....	67
APPENDIX 2.....	71

LIST OF FIGURES

Figure 1. Map of southeastern Mexico.	9
Figure 2. Geologic map of Chiapas Massif Complex.	12
Figure 3. Simplified geologic map of northern part of Oaxacan complex.	14
Figure 4. Geological map of the Guichicovi Complex, showing the distribution of its lithological units.	15
Figure 5. Simplified lithological units of the Guichicovi Complex.	16
Figure 6. Stratigraphic columns of Comalcalco basin, Reforma-Akal Uplift and Macuspana basin.	19
Figure 7. Stratigraphic columns of Comalcalco and Macuspana basin during the Miocene.	19
Figure 8. Detrital composition and classification of sandstones from Comalcalco and Macuspana Basins.	21
Figure 9. Map of southeastern Mexico. The red points represent the location where samples were taken.	22
Figure 10. Stratigraphic position of samples into the Comalcalco and Macuspana basins.	23
Figure 11. Photographs of the outcrops where the samples were taken from Comalcalco and Macuspana basins.	25
Figure 12. Photographs of the techniques used for mineral separation.	27
Figure 13. Photographs of the samples on the EpoFix mounts.	27
Figure 14. Relative percentages of heavy minerals found in the analyzed samples.	30
Figure 15. Heavy minerals found in 6Apr18-3B sample (Amate Formation).	34
Figure 16. Heavy minerals found in 3Apr18-1A sample (Filisola Formation).	35
Figure 17. Heavy minerals found in 2Apr18-5B sample (Encanto Formation).	35
Figure 18. Heavy minerals found in 4Apr18-5A sample (Encanto Formation).	36
Figure 19. Heavy minerals found in 2Apr18-2B sample (Depósito Formation).	36
Figure 20. Heavy minerals found in 4Apr18-3B sample (Nanchital Shale).	37
Figure 21. SEM photos and EDS spectra of Ti-bearing amphibole.	38
Figure 22. SEM photos and EDS spectra of Apatite.	39
Figure 23. SEM photo and EDS spectrum of Chlorite.	39
Figure 24. SEM photos of Chloritoid and its EDS spectrum.	40
Figure 25. SEM photos and EDS spectra of Chromium spinel.	40
Figure 26. SEM photos and EDS spectra of Epidote.	41

Figure 27. SEM photos and EDS spectra of Garnet.	42
Figure 28. SEM photo and EDS spectrum of Ilmenite.	43
Figure 29. SEM photos and EDS spectra of Rutile.....	43
Figure 30. SEM photo and EDS spectrum of Staurolite.....	44
Figure 31. SEM photo and EDS spectrum of Titanite.	44
Figure 32. SEM photos and EDS spectra of Zircon.....	45
Figure 33. Ternary diagram for garnet.....	47
Figure 34. Pattern for the distribution of some heavy minerals toward the basins during Miocene.....	49

LIST OF TABLES

Table 1. Geological unit and outcrop descriptions.....	23
Table 2. Minerals found by Petrographic analysis.....	34
Table 3. Composition of garnets from SEM-EDS analysis (in wt. % of oxides).....	46
Table 4. Relative abundance of garnet end-members (in Mol%).	46
Table 5. Petrographic analysis of 6Apr18-3B sample (Amate Formation, upper Miocene). ...	67
Table 6. Petrographic analysis of 3Apr18-1A sample (Filisola Formation, middle-upper Miocene).....	67
Table 7. Petrographic analysis of 2Apr18-5B sample (Encanto Formation, late lower-middle Miocene).	68
Table 8. Petrographic analysis of 4Apr18-5A sample (Encanto Formation, late lower-middle Miocene).	68
Table 9. Petrographic analysis of 2Apr18-2B sample (Depósito Formation, lower Miocene). ...	69
Table 10. Petrographic analysis of 4Apr18-3B sample (Nanchital Shale, early lower Miocene).	69
Table 11. Group of minerals and some characteristics of them.....	71

1. INTRODUCTION

Study area

The Southeast Basins of Mexico, located in the south coast of Mexico Gulf, are economically significant due to the occurrence of prominent oil and gas resources. Furthermore, the gas production of Mexico is mainly from Miocene sandstone reservoirs of these basins. These basins, also known as Gulf Coast Tertiary basins, were formed as the result of extensive tectonic stress, which was characterized by the influx of a great volume of sediments, gravity sliding of sediments and mobilization of shale masses. The three main basins are included Isthmian Saline, Comalcalco, and Macuspana basins (Chavez et al., 2009), the latter two ones are chosen for the purpose of this research (see Figure 1).

According to Chavez et al. (2009), Miocene sediments of these basins are arkose and subarkose with a lesser proportion of litharenite and lithic arkose. The provenance of these sediments is related to the metamorphic granitic Massif Complex of Chiapas and the Sierra de Chiapas mountain range, both located at the south of these basins. However, the continental terrigenous materials could be sourced by western metamorphic complexes located near to the basins, and/or at least from their reworked material. These complexes are named Grenvillian Oaxacan Complex and Guichicovi Complex.

Sedimentary provenance analysis

The application of heavy minerals is a valuable exploratory tool in studying sediment provenance of geologically complex basins, as the case of Southeast Basins of Mexico (Mange & Wright, 2007). This can assist to reconstruct sedimentary processes since the initial sediment erosion from the parent rock and transport to the deposition and ultimate detritus burial (Pettijohn et al., 1987) as well as the location and nature of sediment sources (Haughton et al., 1991). For instance, in the oil industry, having knowledge of the source/s of rocks in the sedimentary basins is critical to assist determination of the petrological characteristic of rocks and predict oil reservoir characteristics based on studying their stratigraphic units.

According to Planckaert (2005), good oil reservoirs must have a great capacity for storing hydrocarbon fluids; and this depends principally on porosity. To have a suitable porosity, the reservoir rock must have pore network which allows fluid displacement, controlled mainly by the petrological characteristics of the rock. For example, a source area that generates rich-in-quartz detritus during a particular stage of the sedimentary history of the basin, will boost a quartz-rich stratigraphic unit be deposited. This gives rise to a possibly good oil reservoir if additionally, the stratigraphic unit is free-matrix well-sorted, forming a high permeable rock. On the other hand, if arkosic sandstone are deposited in a basin, the alteration of feldspars during diagenesis can lead to a pseudomatrix concealed the porosity, and consequently not good oil reservoir will occur. A sediment is rich in feldspars can be altered and converted into albite and clays, which is not convenient for oil reservoirs because it plugs the pore rock network, making difficult the storing and passing of oil into the rock (Wonder & Morad, 2000). Therefore, it is essential to precise the provenance of the sediments.

Limitations related to the reliability of the use of heavy mineral as provenance indicator exist. When heavy minerals are released from their source rocks, several processes occur until they are taken off from the sediments (Mange & Maurer, 1992). The influence of these processes may disturb the trustworthiness of sedimentary provenance studies. The most significant modifying factors are followed (Mackie, 1923; van Andel, 1959; Blatt, 1967; Humbert, 1971; Pettijohn et al, 1973; Morton, 1985a). 1) The Climate of the source area, influences weathering process into the source rock, and this may chemically alter minerals; thus, the original input of heavy minerals into the sediments will be disturb; 2) Abrasion and Mechanical Damage during the transport of heavy mineral assemblages, that depends on the mechanical durability of the minerals. In general, mechanical changes make less significant modifications (Russel 1937, Shukri 1949), mostly influencing the shape of grains; 3) The Hydraulic Factor at the minerals transport produces a grain selection based on its size, form, and density of the minerals; 4) The Post-depositional Diagenetic Effects, where the elimination of the less resistant grains occurs, that influences the final heavy mineral assemblages into the sediment packages (Mange & Maurer, 1992).

To analyze detrital heavy minerals, several techniques can be used. Typically, the petrographic studies as an indispensable and first tool can provide valuable preliminary information of the type and abundance of heavy minerals. In addition, geochemical methods using micro-analytical

techniques such as scanning electron microscopy (SEM) can be used with greater expense involved.

In the current study, the heavy minerals from Southeast sedimentary basins of Mexico are studied by petrographic and micro-analytical (SEM) techniques. This approach can be potentially applied in similar sedimentary basins of Ecuador. According to HAO et al. (2018), Ecuador has the third largest proven oil reserves in South America, located in the Oriente and Guayaquil basins. There are many oilfields, the largest one located in the Oriente basin (named Sacha oilfield), that store 0.4 billion tons of proven oil reserves. Using sediment provenance techniques may help to provide new reservoir oil prospects in Ecuador and enlarge the oil exploration and production in this country.

Problem statement

Macuspana and Comalcalco basins are reservoirs of prominent oil and gas resources. The limited work has been done in this area to analyze the provenance of the Paleogene and Neogene sediments (Chavez et al., 2009). The deformation of Sierra de Chiapas occurred in Palaeocene–Eocene, which was coeval to the depocentre formation of the Tabasco coastal plain. This coastal plain includes Macuspana and Comalcalco basins territory. According to Brichau et al. (2008), the Palaeocene–Eocene terrigenous rocks of Sierra de Chiapas (see Figure 1) have a northwestwards source. Also, Weber & Hecht (2003) suggested that these rocks were mostly sourced from the Grenvillian Oaxaca and the Guichicovi complexes. In addition, it is possible that Miocene sandy stratigraphic units of the Macuspana and Comalcalco basins were sourced by the Grenvillian Oaxaca and the Guichicovi complexes and/or at least from their reworked materials; a sediment provenance analysis becomes necessary to solve this hypothesis. Therefore, this research addresses the provenance of Miocene sandstone reservoirs, which helps to evaluate the occurrence of new probable rock reservoirs. Furthermore, in 1986, Nazareth oilfield was discovered within the petroleum province of Sierra de Chiapas, that is composed by a mixed fossiliferous Paleocene sediments- clastics- calcareous of the main platform (González, 2001).

Objective

This project aims to determine the provenance of the Miocene sediments deposited in the Comalcalco and Macuspana basins from Southeastern basins of Mexico, using petrographic and chemical analysis of heavy minerals suite present in those sediments.

2. DETRITAL HEAVY MINERALS

Detrital heavy minerals are defined as minerals with a high density ($>2.85 \text{ g/cm}^3$). They could be both essential minerals in their host rock, such as amphibole or mica mineral groups, or accessory phases such as apatite or zircon (Mange & Maurer, 1992). In siliciclastic sediments, heavy minerals typically comprise 1% of the rock volume (Mange & Wright, 2007). Below, the heavy mineral of this study are described.

1. Amphibole (Ti-bearing)

Ti-bearing amphibole is a mineral of igneous origin. It is common as phenocrysts in alkaline volcanic rocks, gabbroic and peridotitic nodules in alkaline basalts, syenites, monzonites, carbonatite tuffs, and alkaline gabbros (John et al., 2001).

2. Apatite

Apatite is a common accessory mineral of almost all igneous and hydrothermally metamorphosed rocks (Weissbrod & Nachmias, 1986; Piccoli & Candela, 2002). It typically occurs in igneous rocks such as felsic (e.g., andesite to rhyolite volcanic rocks, and their plutonic equivalents), mafic (e.g., basalts and their plutonic equivalents) and ultramafic rocks. Also, apatite is widespread in sedimentary rocks such as sandstones as detrital grains because of its high chemical stability (Mange & Maurer, 1992).

3. Chlorite

Chlorite is a common mineral in low-medium grade metamorphic rocks and more commonly present in the greenschist facies. In igneous rocks, this mineral is formed by hydrothermal alteration of ferromagnesian minerals such as biotite. Also, it can be formed by weathering processes or formed authigenically during diagenesis in sedimentary rocks (Mange & Maurer, 1992).

4. Chloritoid

Chloritoid is a common mineral in low- to medium-grade metapelites of various pressure conditions (Deer et al., 1992). Also, it can be formed by hydrothermal processes in veins and

cavity fillings (Mange & Maurer, 1992). It is a stable mineral, similar to garnet in the sedimentary cycle (Morton, 1985a).

5. Chromian spinel

It is a widespread accessory mineral in mafic rocks (Dick & Bullen, 1984), and according to Roeder & Poustovetov (2001) it is commonly found in mid-ocean ridge basalts (MORB). It is also a widespread accessory mineral in several types of ultramafic rocks such as peridotites (Mange & Maurer, 1992). Chromian spinel cannot be formed authigenically in sediments (Press, 1986). It is frequent in sediments sourced by ophiolitic rocks (Mange & Maurer, 2012). Furthermore, according to Zimmerle (1984) chromian spinel has a geotectonic significance because there is an increase of this mineral in sediments during orogenic periods.

6. Epidote

Epidote occurs in regional metamorphism environment related to various metamorphic facies such as greenschist and epidote-amphibolite facies (Deer et al., 1982). In igneous rocks, this mineral is more common in the basic ones, but may also occur in granites (Asiedu, 2000).

7. Garnet

Garnet group minerals are characteristic of metamorphic rocks (e.g., schist, gneiss, or marble), but also can be found in peridotites and kimberlites, as well in evolved felsic volcanic rocks such as granites and pegmatites. In sediments, garnet minerals are present as detrital grains due to their resistance to abrasion and chemical attack during the sedimentary cycle (Deer et al., 1982; Suggate & Hall, 2014). The use of chemical composition of garnet is a trustworthy way to reconstruct source rock and provenance (Morton, 1985a). It can be expressed as percentage of the 'garnet end-members' which form two solid solution series: the pyrope group (pyrope, almandine and spessartine) and the ugrandite group (uvarovite, grossular, and andradite) (Suggate & Hall, 2014).

8. Ilmenite

Ilmenite is an opaque accessory mineral in most rocks with granitic–tonalitic composition, amphibolites, high-grade metamorphic rocks such as charnockites and sillimanite–kyanite bearing metasediments (Bernstein et al., 2008).

9. Rutile

Rutile forms predominantly in metamorphic conditions, being more common in metapelites (Luvizotto & Zack 2009). In particular, it can be found in schists, gneisses and amphibolites and is more abundant in higher-pressure metamorphic rocks compared to those lower-pressure ones (Zack et al. 2002). Rutile in igneous rocks appears in hornblende-rich plutonic types and pegmatites (Mange & Maurer, 1992). In clastic sediments, rutile is commonly present due to its great resistance to weathering, transport, and diagenesis (Hubert 1962; Morton & Hallsworth 1994). Furthermore, rutile may be present as an authigenic mineral in sediments, forming thin laths or clusters of needles, often intergrown with other Ti-bearing phases (Mange & Maurer, 1992).

10. Staurolite

Staurolite is mostly formed in medium-grade regional metamorphic conditions, seen in mica schists derived from argillaceous sediments, and less frequently in gneisses (Mange & Maurer, 1992).

11. Titanite

Titanite is a typical accessory mineral in igneous rocks. Deer et al. (1982) indicated that in basic and ultrabasic igneous rocks, titanite is closest to the theoretical CaTiSiO_5 composition, whereas in acidic and intermediate rocks, it contains a significant amount of Fe, Al and rare earth elements (Asiedu, 2000). It is not a very common phase in volcanic rocks compared to plutonic rocks. Generally, titanite is a widespread accessory mineral in pegmatites. Referring to metamorphic rocks, titanite occurs in amphibolite facies rocks, gneiss and schists rich in ferromagnesian minerals (Mange & Maurer, 1992). Metamorphic and skarn titanite is generally characterized by higher Al contents (up to 10 wt. % Al_2O_3) compared to igneous titanite (Asiedu, 2000). Titanite is a chemically unstable phase and usually dissolves at an early stage of diagenesis (Mange &

Maurer, 1992). Therefore, it is not easily observed as a detrital mineral in sediments even when the source of those sediments had it.

12. Zircon

Zircon is a widespread accessory mineral in rocks of crustal origin. It is especially abundant in silicic and intermediate igneous rocks. It also forms in mantle xenoliths (Mange & Maurer, 1992). Because of its high resistance to weathering and diagenesis, it is commonly a detrital mineral in sediments.

3. GEOLOGICAL FRAMEWORK

The southeast structures of Mexico are located between the Chiapas Massif Complex to the southwest and the Yucatan platform to the northeast. According to Meneses-Rocha (2001), these structures are divided into two tectonic domains: the northwest-oriented Neogene fold-and-thrust belt, and the northeast-oriented Gulf Coast Tertiary basins (see Figure 1).

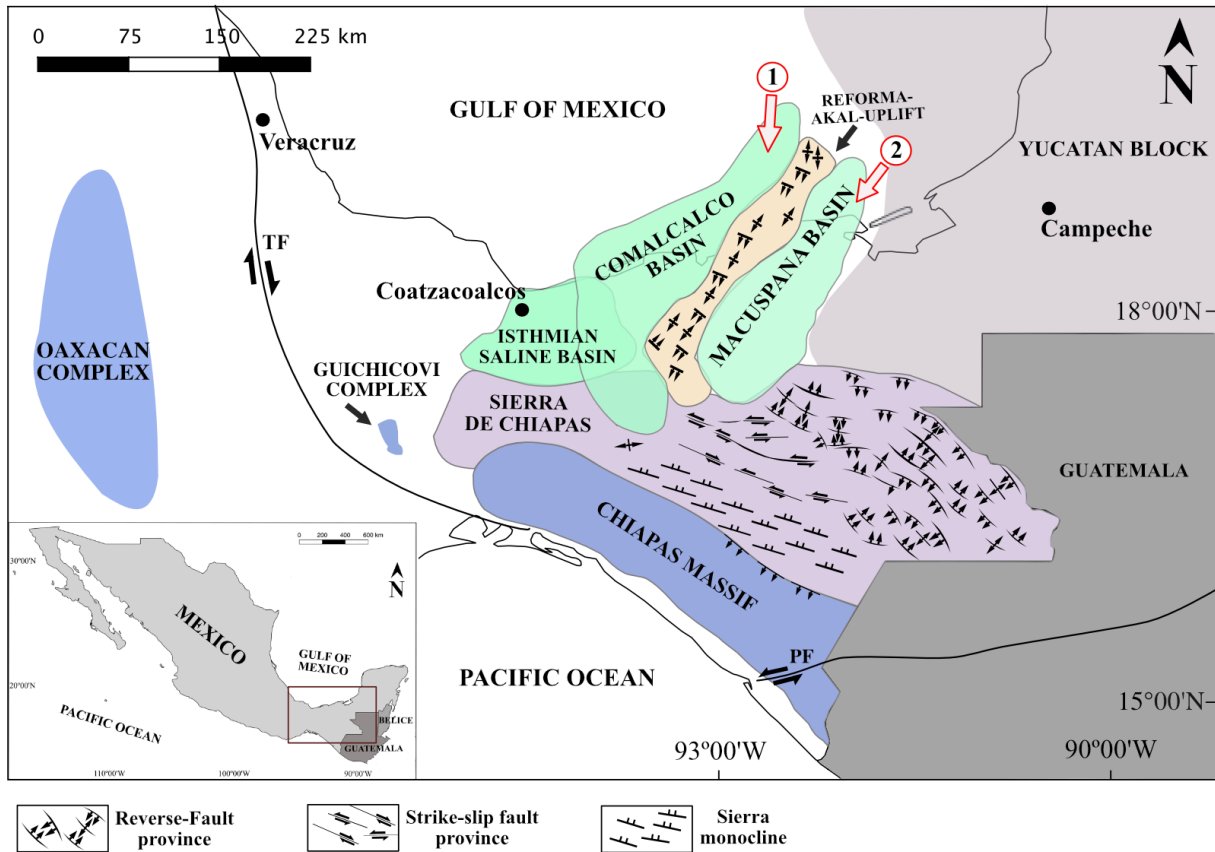


Figure 1. Map of southeastern Mexico. The red arrows show the basins in which this study is focused and the blue polygons represent the complexes that are possible source rock for those basins. PF: Motagua- Polochic Fault and TF: Tamaulipas-Oaxaca Transform Fault, both major fault zones. Adapted from Keppie et al., 2001; Meneses-Rocha, 2001; Padilla y Sánchez, 2007; Nieto-Samaniego et al., 2006; Weber et al., 2007, 2018.

The Neogene fold-and-thrust belt is formed by Sierra de Chiapas and Reforma-Akal Uplift. The Sierra de Chiapas has more than 300 km of mountains aligned parallel to the Pacific coast being 80 km wide; the altitude varies from 900 to 3,000 m near of Guatemala (Rosales-Domínguez, 1997; González-Lara, 2001). It is divided into three main tectonic provinces: Strike-slip fault province, Reverse-fault province, and Sierra Monocline. The Reforma-Akal Uplift is located

between the Comalcalco and Macuspana basins. In this uplift, there are huge petroleum-bearing anticlines (Meneses-Rocha, 2001).

The Northeast-oriented Gulf Coast Tertiary basins are Macuspana, Comalcalco, and Isthmian Saline basins. The Macuspana basin is bounded by the Sierra de Chiapas in the south, the Yucatan platform in the east, the Reform-Akal in the west, and the Gulf of Mexico in the north (Ambrose et al., 2003). The Comalcalco basin is bordered in the southwest by the Isthmus Saline basin and in the east by the Reforma – Akal uplift that separates it from the Macuspana basin (Meneses-Rocha, 2001). The Isthmian Saline basin extends from the Sierra de Chiapas into the continental shelf of the Gulf of Mexico, and in the east, is bounded by the Comalcalco basin (Meneses-Rocha & Bartolini, 2001).

Tectonism of the study area

Two main fault systems have influenced the southeast of Mexico, including: the Tamaulipas-Oaxaca and Motagua-Polochic faults. Along the Tamaulipas-Oaxaca Transform fault, accommodation of the counterclockwise rotation of the Yucatán-Chiapas block occurred, which comprises the terrains located at the right of the Tamaulipas-Oaxaca Transform fault. This movement began approximately 49° in the Middle Jurassic (165 Ma) until the end of the Callovian (163.5 Ma), when it changes to vertical movement acting as a system of normal faults (Padilla y Sanchez, 2007). The Motagua-Polochic Transform Fault separates the North American Plate to the North from the Caribbean plate to the south (Weber et al., 2007), and initiated its movement in early Cenozoic to Neogene; it is active to the present (González-Lara, 2001; Padilla y Sanchez, 2007) and explains the current deformation of Sierra de Chiapas.

Metamorphic complexes of Southeast of Mexico

There are three metamorphic complexes in the south of Mexico. These are located at the south and west of the Northeast-oriented Gulf Coast Tertiary basins (see Figure 1). They are named Chiapas Massif Complex, Oaxacan Complex, and Guichicovi Complex.

Chiapas Massif Complex is dominated by deformed granitoids including those of granite composition (Schaaf et al., 2002; Weber et al., 2007) and these rocks have a high content of

quartz which helps to create a high permeable rock, characteristic essential in hydrocarbon reservoir rocks. A similar process to form sandy reservoirs is referred by Duarte et al. (2018) for the Aptian sediments in the upper Magdalena Valley, in Colombia. On the other hand, the Grenvillian Oaxacan Complex is dominantly formed by calc-pelitic paragneiss (Ortega-Gutierrez, 1981) and the Guichicovi Complex is dominantly formed by felsic gneisses, which are feldspar-rich rocks (Weber & Hecht, 2003). Chiapas Massif Complex, compared to the Oaxacan and Guichicovi complexes, seems to be the most beneficial source in order to contribute with useful sediments to originate a good hydrocarbon reservoir. Grenvillian Oaxacan and Guichicovi complexes contribute mostly with very fine sediments and feldspars respectively; with diagenesis, they may form a pseudomatrix that block out the necessary porosity to originate a good oil reservoir.

Chiapas Massif Complex (CMC)

The Chiapas Massif Complex (CMC) is the largest Permian batholithic complex in Mexico, covering an area of 20,000 km² in southeastern Mexico. It is dominated by deformed granitoids (granite to minor gabbro in composition) intruding orthogneiss, amphibolites, and metasedimentary rocks (Schaaf et al., 2002; Weber et al., 2007) including metapelites and calcsilicate rocks (Weber et al., 2007) (see Figure 2). There are garnet amphibole gneisses. The chemical composition of amphibolites is comparable to those from typical E-MORBs (evolved mid-ocean ridge basalt; Weber et al., 2018). The formation of this complex began principally at ~272 Ma in the Early Permian, with the intrusion of orthogneiss protoliths, and finished at ~254–250 Ma in the Late Permian, with medium- to high-grade metamorphism, anatexis, and intrusion of magmatic bodies (Weber et al., 2007).

El Triunfo Complex

El Triunfo Complex is part of the CMC, located in the southeast of CMC, where the Permian plutons are minimal relative to the Ordovician igneous rocks (Estrada-Carmona et al., 2012; Weber et al., 2008) and the massif-type anorthosites are associated with several beds (up to ten meters in thickness) of rutile-bearing ilmenitites. El Triunfo Complex was intruded by E-MORB magmas (Weber et al., 2018).

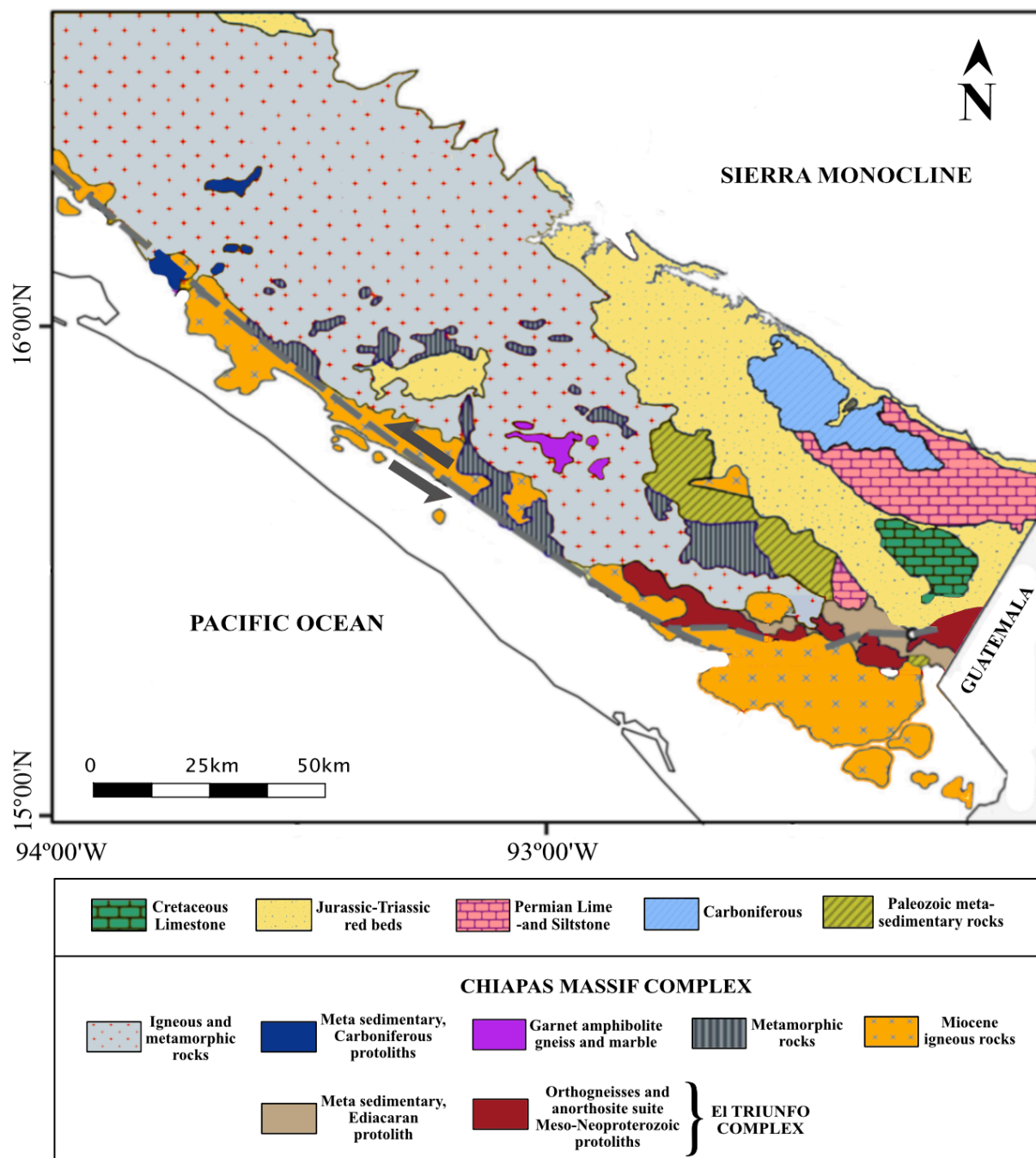


Figure 2. Geologic map of Chiapas Massif Complex. Adapted from Weber et al. (2018).

Grenvillian Complexes

In the state of Oaxaca, west and southwest of the Chiapas state, there are two Grenvillian complexes: Oaxacan and Guichicovi. They have similar geological features, such as the granulite facies metamorphism and a 1.0 Ga orogenic event (Ortega-Gutiérrez et al., 1995).

Grenvillian Oaxacan Complex

According to Ortega-Gutiérrez (1981), the Grenvillian Oaxaca Complex (Figure 3) is a large Precambrian basement complex (1Ga) exposed along a 50-100 km-wide belt trending NNW-SSE in the central part of the state of Oaxaca. It is a meta-anorthosite massif (magmatic in origin) of intermediate composition, with andesine plagioclase as the dominant mineral. Orthogneisses (100 to 2000 m thick) are located on top of the anorthosites and have ultrabasic to ultrafelsic composition. The lower part of orthogneisses is composed of bands and lenses of ilmenite-magnetite-apatite (nelsonite) and apatite-ilmenite-rich gneisses, which are interbanded with the anorthosites; whereas the upper part is composed mostly of gabbroic to granitic garnetiferous rocks. The orthogneiss is surrounded by a paragneissic sequence, its lower part consists of Ca-rich banded gneisses with marble and scapolite-rich calcsilicates, and its upper part formed mostly by pelitic gneisses rich in garnet, sillimanite and biotite, and charnockitic banded gneisses (Ortega-Gutiérrez, 1981). The complex is intruded by a post-metamorphic Middle Triassic granitic pluton, 240 ± 30 Ma in age (Fries et al., 1966).

Protoliths of the gneissic rocks are sedimentary rocks and felsic (charnockitic-syenitic-enderbitic) to intermediate- gabbroic (jotunitic to noritic) rocks with abundant accessory phases such as zircon, apatite, allanite, and titaniferous oxides (Keppie et al., 2001). These rocks were metamorphosed at granulite facies (Kesler, 1970, 1973; Ortega-Gutiérrez, 1984; Mora et al., 1983; Solari et al., 1998), including intermediate pressure (5-8 Kbar) and high temperature (700-800 °C) (Ortega-Gutierrez, 1981; Mora and Valley, 1985). This metamorphism may have occurred during the intrusion of the gabbroic-anorthositic magmas or as a result of the continental collision event of the Grenville Orogeny (Ortega-Gutierrez, 1981). The granulite facies were followed by amphibolite and greenschist facies metamorphism (Keppie et al., 2001).

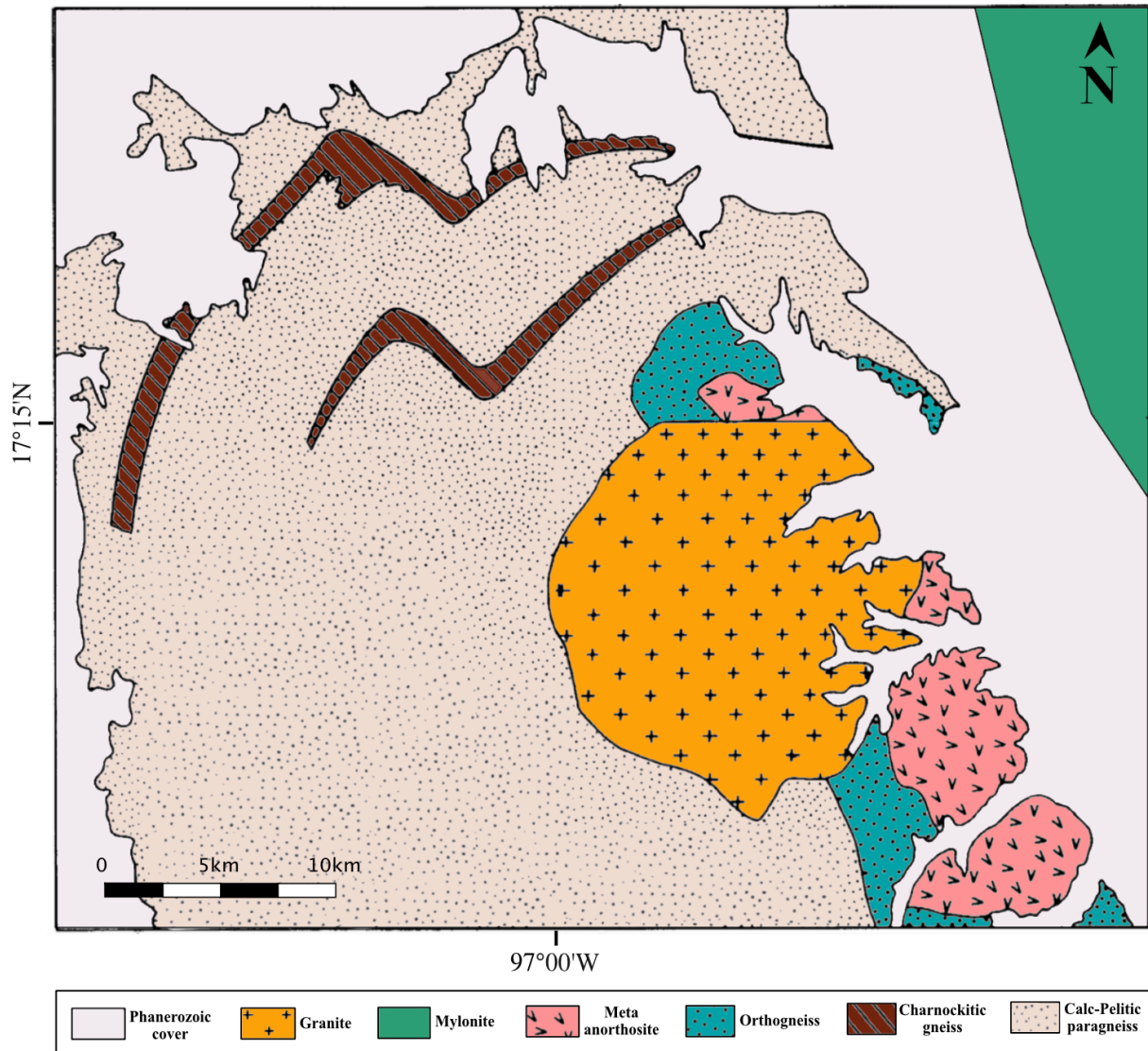


Figure 3. Simplified geologic map of northern part of Oaxacan complex. Adapted from Ortega-Gutiérrez (1981).

Guichicovi Complex

The Guichicovi Complex is a high-grade metamorphic crystalline complex (Weber & Köhler, 1999), which covers an area of about 800 km². It consists of metaigneous rocks in the west and north, and mainly metasedimentary series (supracrustals) in the east (see Figure 4). The metasedimentary sequences comprise garnet- and/or biotite-rich quartz-feldspathic gneisses (likely of magmatic origin) interlayered with graphite-rich paragneisses, intercalated with gabbroic dikes and pegmatites (Weber & Hecht, 2003).

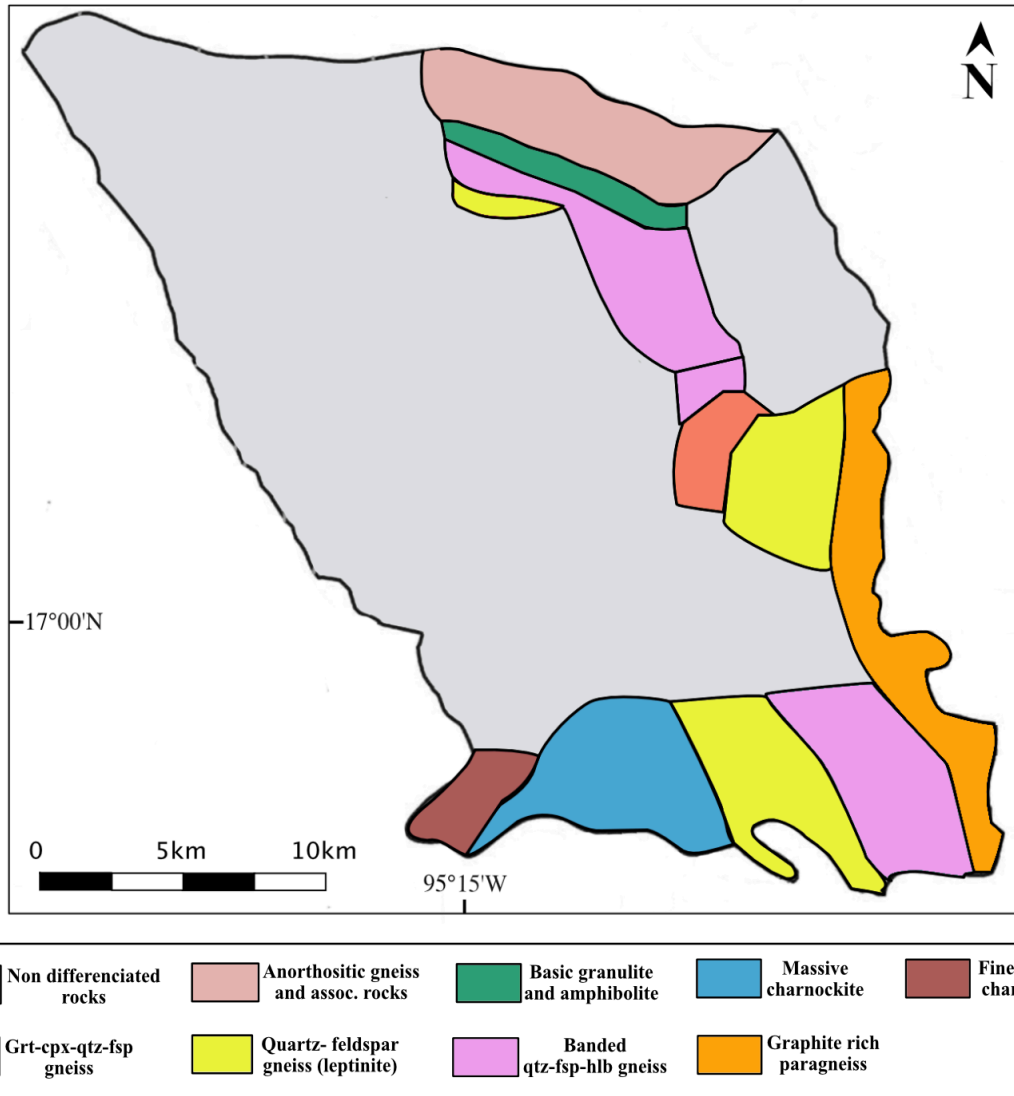


Figure 4. Geological map of the Guichicovi Complex, showing the distribution of its lithological units. Adapted from Weber & Köhler (1999).

The Guichicovi igneous rocks are divided into two major lithologic units (see Figure 5): 1) the Northern Guichicovi Unit, which includes anorthositic-tonalitic gneisses, granulites of mafic composition, and hornblende gneisses; 2) the Southern Zacatal Unit, including granulites of felsic composition and orthogneisses (Weber & Hecht, 2003).

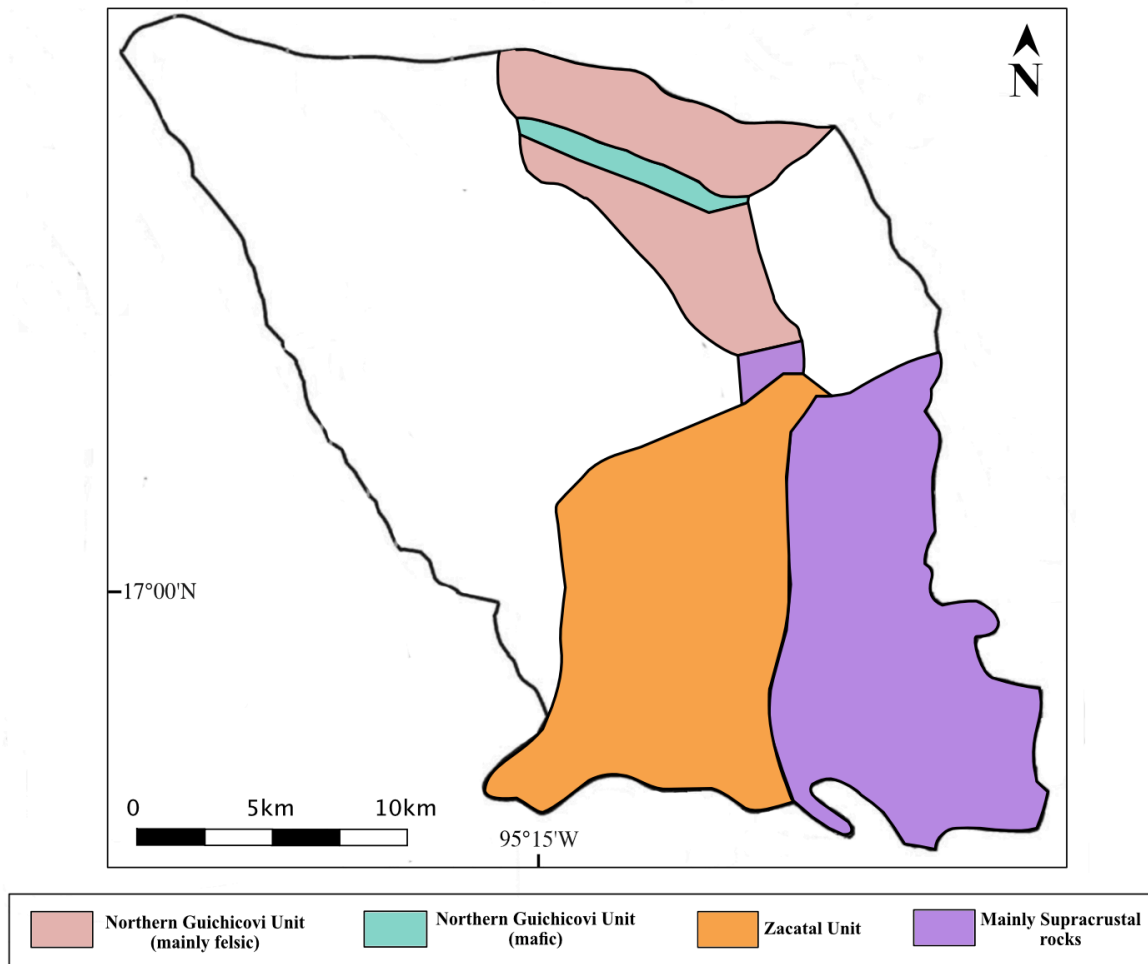


Figure 5. Simplified lithological units of the Guichicovi Complex. Adapted from Weber & Hecht (2003).

1) The *Northern Guichicovi Unit* consists of anorthositic-tonalitic gneisses. Towards the south, there are mafic granulites and continuing to the south, the hornblende gneiss (Weber & Hecht, 2003). The leucocratic *Anorthositic-Tonalitic Gneisses* are leucocratic (white to greenish) plagioclase-rich, fine to medium-grained, granoblastic with gneissic texture. These are intercalated with dm-wide paragneiss layers, which suggests that anorthositic-tonalitic dikes and sills intruded the sedimentary units. Titanite is abundant in these gneisses and generally replaces Ti-oxide minerals completely (Weber & Hecht, 2003). The *Granulites of Mafic composition* are fine to medium-grained with granular texture in which garnet is the dominant phase, exceeding 30% of the modal composition. These granulites are composed of: garnet, clinopyroxene, plagioclase, and \pm quartz assemblage; and biotite and titanite are later secondary phases. Also, they have abundant opaque minerals, mainly: ilmenite, sulfide ores, and may include magnetite. In some granulites, garnets, and pyroxenes were partially retrogressed to green amphibole,

transforming them into an amphibolite (Weber & Hecht, 2003). The *Hornblende Gneisses* are medium-grained foliated rocks. They have green hornblende and plagioclase as dominant minerals (Weber & Hecht, 2003).

2) The *Zacatal Unit* is composed of garnet-bearing quartz-feldspathic orthogneisses. The felsic orthogneisses are medium- to coarse-grained, granoblastic with or without foliation, composed principally of perthitic K-feldspar, quartz, and plagioclase (oligoclase - andesine). The most abundant mafic mineral is brown hornblende (amphibole), which is rich in titanium. Zacatal Unit contains numerous pegmatites with megacrysts of micas, which intruded into graphite-rich paragneisses (Weber & Hecht, 2003).

The metamorphism of Guichicovi Complex occurred under P - T peak conditions of 7.4 ± 0.3 Kbar and 837 ± 59 °C (Murillo-Muñeton and Anderson, 1994), at 986 ± 4 Ma ago (Neo-Proterozoic, Ruiz et al., 1999). Then, this Complex was intruded by Permo-Triassic and Jurassic granitoids (Damon et al., 1981; Murillo-Muñetón, 1996; Weber, 1998).

Macuspana and Comalcalco basins

The origin of the Southeast Basins of Mexico is intimately linked with the Sierra de Chiapas and the Reforma-Akal folded chain. According to Ambrose et al. (2003), during the Oligocene, clastics were deposited throughout the Mexican southeast. At this time, in the Macuspana area, a depocenter began to be developed and thick clay sequences were deposited. Coeval to this, in the area of Comalcalco- Isthmian Saline the mobilization of large volumes of salts (deposited at 166 Ma, in the Callovian) began (Ángeles-Áquino et al., 1992).

Macuspana and Comalcalco basins formed as the result of an extensive tectonic activity that occurred since the middle Miocene (Serravalian, 12.0 Ma). The opening of these basins is related to a great compressional deformation stage at 12.0 Ma (Serravalian) which folded the rocks of the Chiapas-Reforma-Akal Chain (Padilla y Sánchez, 2007). This period is known as Chiapaneca orogenic phase (Chavez et al., 2009). At the end of the Miocene, as an extensional effect of this orogenic phase, the tipping of Chiapas-Reforma-Akal chain occurred towards the north due to the evacuation of large volumes of Callovian salt in the same direction (Padilla y Sánchez, 2007).

This caused the opening of the Macuspana basin and its detachment level appears to be at the Callovian salt. Subsequently, the Comalcalco basin opened as a surface extensional scar (Pindell & Miranda, 2011) on a middle Miocene shaly horizon or the Callovian salt (Meneses-Rocha, 2001). The overload of sediments generated great listric synthetic and antithetical normal faults in the Macuspana and Comalcalco basins (Padilla y Sánchez, 2007) that trend perpendicular to the northwest strike of the compressional structures within the Reforma-Akal uplift (Meneses-Rocha, 2001).

In the lower Miocene succession of the Comalcalco basin, terrigenous clastics were accumulated. These sediments were probably deposited in a deltaic environment (Meneses-Rocha, 2001) and during the upper Miocene, this basin was filled with thick delta front sands (Chavez et al., 2009). In the Macuspana basin, from southwest to northeast, its sedimentary facies vary from fluvial-deltaic to transitional marine and turbidite deposition and there are shale ridges, salt diapirs, and argillaceous domes in its central part (Chavez et al., 2009). In the lower Miocene, shaly, deep-water systems are recorded, while in the upper Miocene, shallow-marine and lower-coastal-plain systems are recorded, which is formed by a series of upward-coarsening sandstones. The uppermost upper Miocene section is formed by retrogradational deposits. Also, there are abrupt changes in the sandstone stacking patterns commonly at the base of upward-fining sandstones (Ambrose et al., 2004). Both basins were filled by a great volume of siliciclastic materials due to great contribution of clastics from the Chiapas Massif Complex during the Pliocene and the Pleistocene (Padilla y Sánchez, 2007).

Herein, this research is focused on the Miocene stratigraphic units of the Comalcalco Basin and on the upper Miocene units of the Macuspana Basin. The general stratigraphy of these basins is presented in Figure 6 and the stratigraphy of the basins during the Miocene is presented in Figure 7, accompanied by the stratigraphic units deposited during that time.

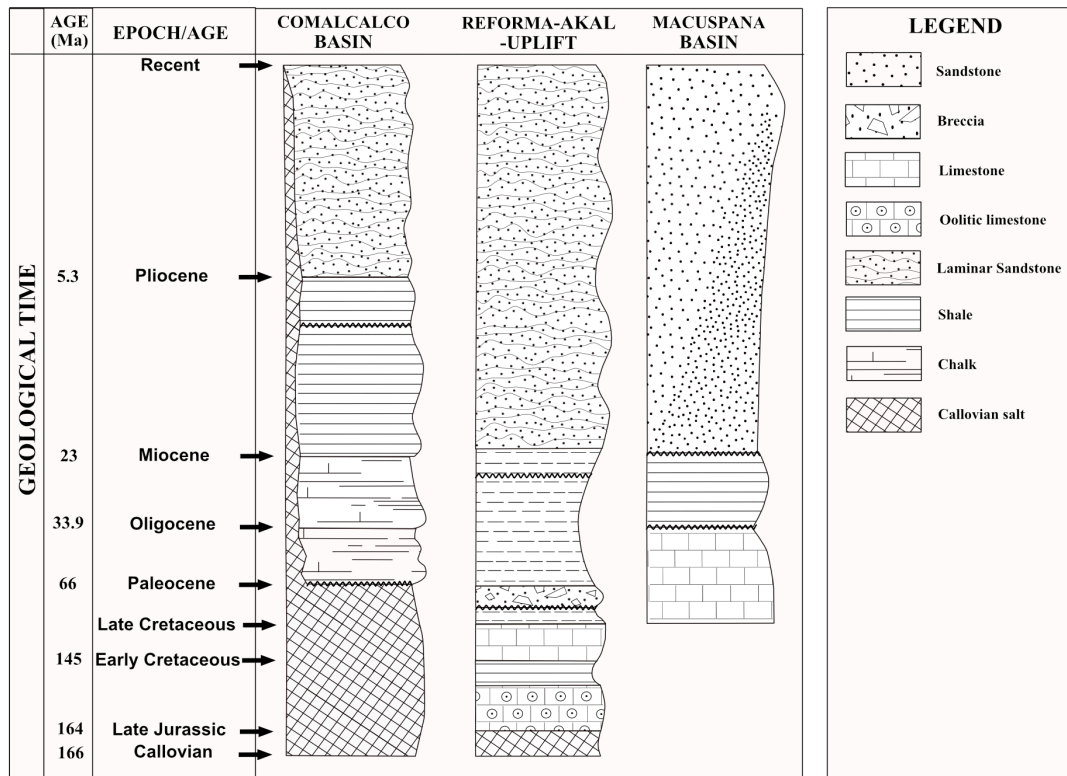


Figure 6. Stratigraphic columns of Comalcalco basin, Reforma-Akal Uplift and Macuspana basin (see Figure 1 for their location). Adapted from Meneses-Rocha, 2001.

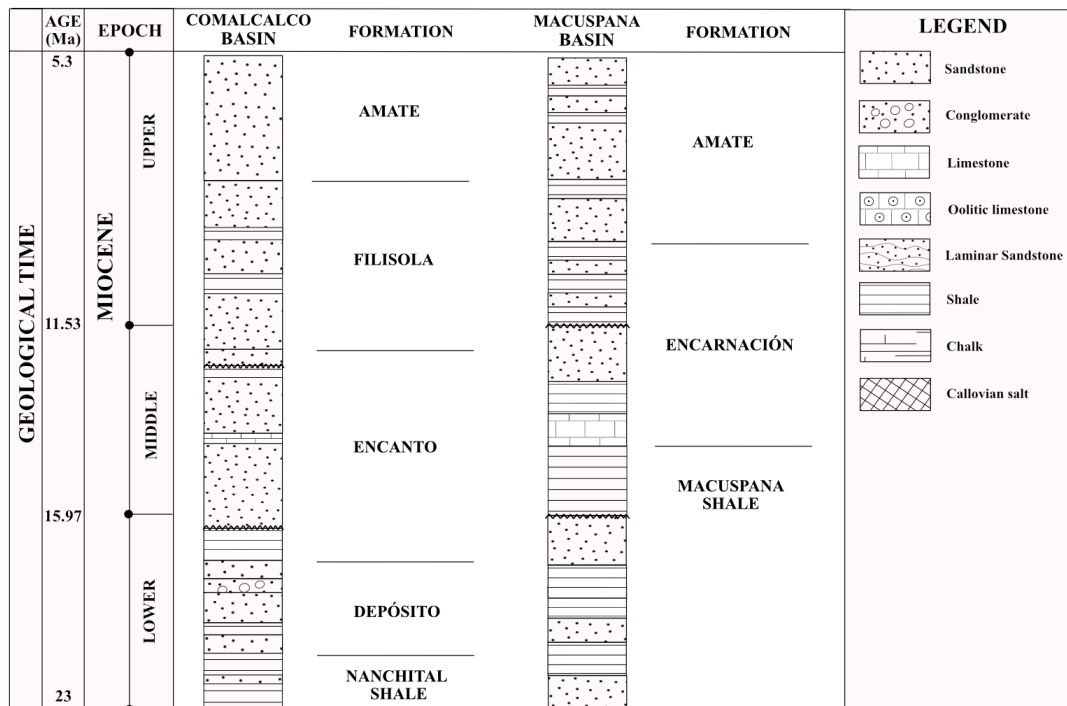


Figure 7. Stratigraphic columns of Comalcalco and Macuspana basin during the Miocene. Adapted from Narváez-Rodríguez et al., 2008 and from Servicio Geológico Mexicano, 2008.

During the late Paleocene-early Eocene occurred the uplifting of the granitic Chiapas Massif deriving fine to coarse-grained sediments to the Chiapas depression, generating a lateral change of facies, open marine to the west, and internal platform to the upper shore face to the east, a sedimentary regime persisting up to the Plio-Pleistocene, just the fosses infilling (González-Lara, 2001).

The sediments of Comalcalco and Macuspana basins are arkose and subarkose with a lesser proportion of litharenite and lithic arkose (Figure 8), having metamorphic and volcanic provenance. The provenance areas have been established in the Chiapas Massif Complex and the Sierra de Chiapas (Chavez et al., 2009) based on the detrital composition for Paleogene and Neogene sediments. It is reported that the Oligo-Miocene pure continental-type sedimentation has been directly related to uplift and subsequent erosion of the Chiapas Massif Complex (Carfentan, 1985; Meneses-Rocha, 2001). However, the continental terrigenous material towards the Sierra de Chiapas during the Neogene is not solely related to the uplift of the Chiapas Massif Complex (Witt et al., 2012); they could be derived from the Grenvillian Oaxacan and the Guichicovi complexes (Weber & Hecht 2003). As the deformation of Sierra de Chiapas was contemporaneous to the depocentre formation of Macuspana and Comalcalco basins (Brichau et al., 2008), in these basins also could have occurred the same changes in the source area as the case of Sierra de Chiapas.

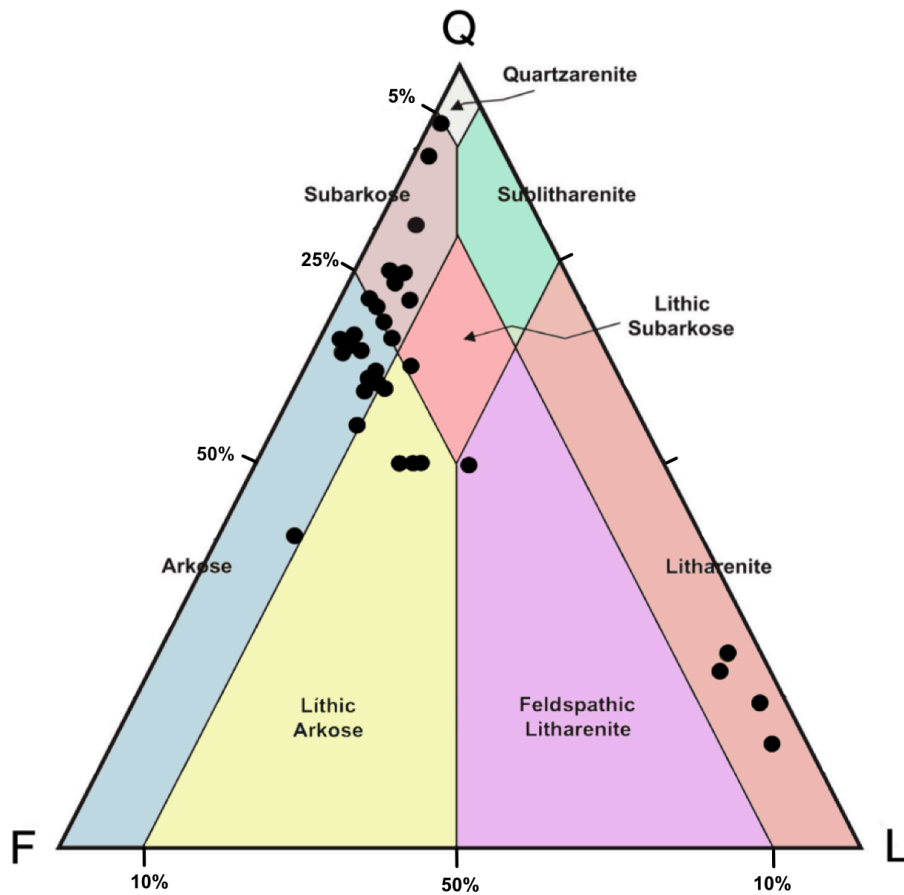


Figure 8. Detrital composition and classification of sandstones from Comalcalco and Macuspana Basins. Q: Quartz, F: Feldspars, L: Lithics. Adapted from Chavez et al. (2009).

Furthermore, U–Pb analysis of single zircons on Palaeocene–Eocene terrigenous rocks of Sierra de Chiapas defined a northwestwards provenance of sediments (Brichau et al., 2008). The 0.8–1 Ga clusters suggest that Palaeocene–Eocene sedimentary units were mostly sourced from basement exposures such as the Grenvillian Oaxacan Complex, or the Guichicovi Complex (Weber & Hecht 2003), most probably eroded during the Laramide orogeny (Nieto-Samaniego et al., 2006).

3. LOCATION OF THE STUDY AREA

Sampling location

In the current study, six samples are taken from the locations defined on the map (see Figure 9). Five samples belong to Depósito, Encanto, Filisola, and Nanchital Shale formations from the Comalcalco basin and one sample from Amate Formation from the Macuspana basin (see Figure 10). A detailed petrological and sedimentological description of the samples is presented in Table 1. The samples are lithic sandstones, lithic arkoses, and arkosic sandstones (see Figure 11).

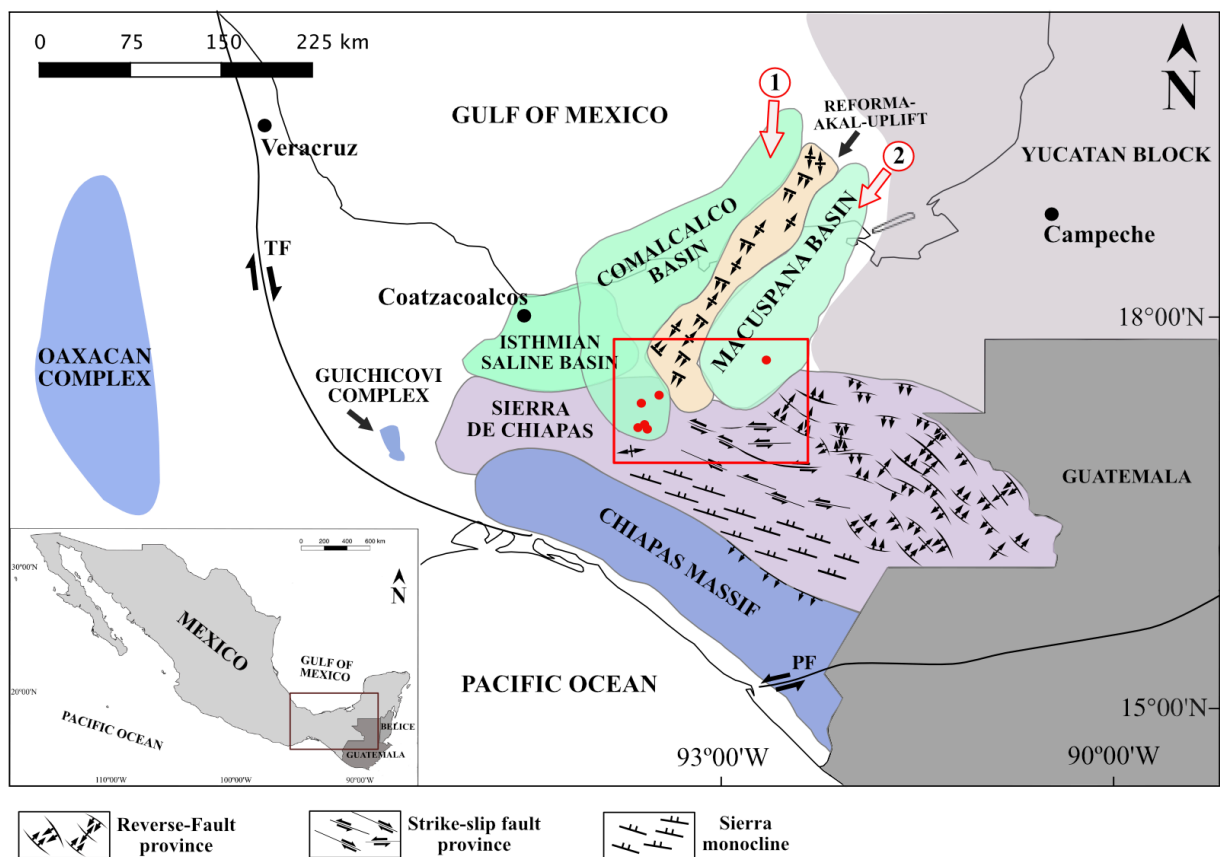


Figure 9. Map of southeastern Mexico. The red points represent the location where samples were taken. Adapted from Meneses-Rocha, 2001; Padilla y Sánchez, 2007; Nieto-Samaniego et al., 2006; Weber et al., 2018; Keppie et al., 2001.

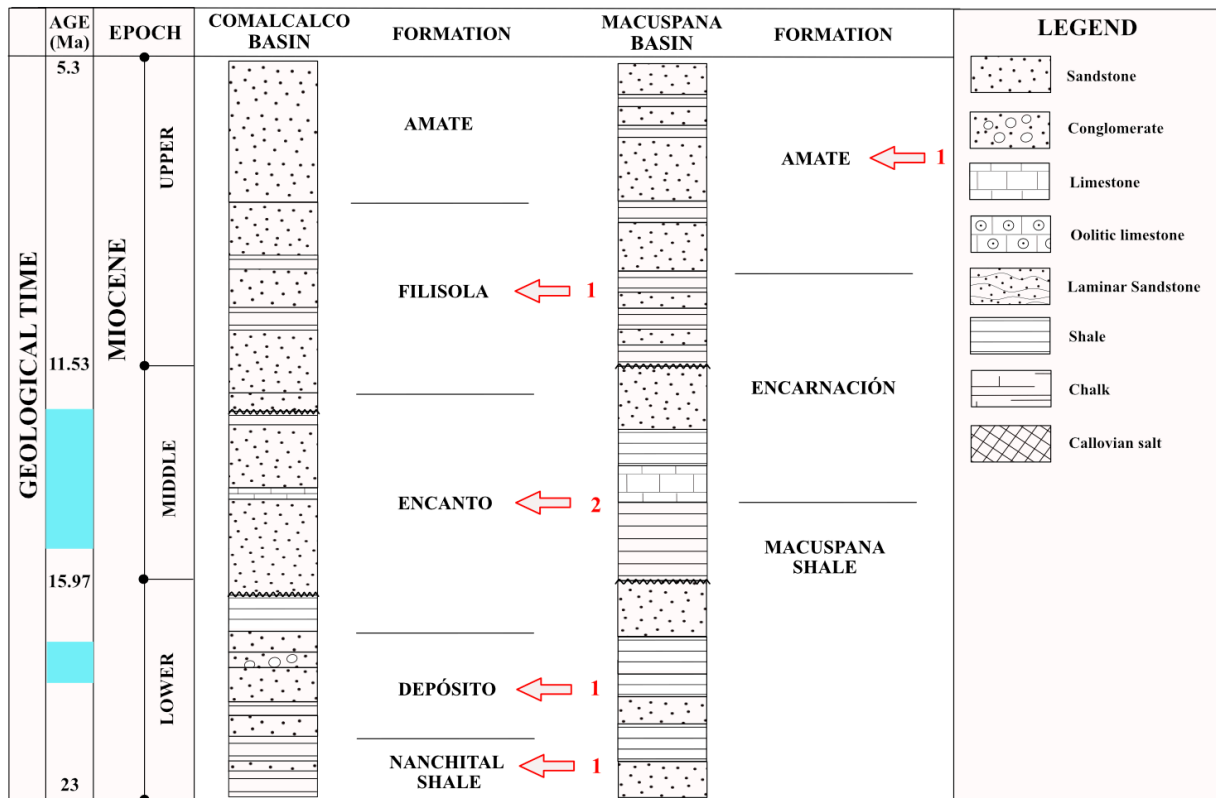


Figure 10. Stratigraphic position of samples into the Comalcalco and Macuspana basins. The red arrows show from which formation samples were taken and the numbers indicate how many sample were taken. Light blue rectangles represent marine incursions. Adapted from Narváez-Rodríguez et al., 2008; and from Servicio Geológico Mexicano, 2008.

Table 1. Stratigraphic Unit and outcrop descriptions.

Sample	Stratigraphic-Unit	Outcrop description	Sample lithology and texture	Hand specimen description
6Apr18-3B	Amate Formation	Outcrop of approx. 2m thick medium-grained calcareous sandstone, with bioclasts of bivalves and gastropods of approx. 5 cm. Composition: quartz, bioclasts, white micas, and black grains.	Medium-grained lithic sandstone	Medium-grained sandstone with quartz, white micas, and bioclasts.
3Apr18-1A	Filisola Formation	Massive coarse-grained sandstones, pebbly sandstones, and shales. Composition of the pebbles in the sandstones are quartz, quartzite, and potassium feldspar.	Coarse grained sandstone	
2Apr18-5B	Encanto Formation	Coarse-grained to pebbly sandstones, with rhyolites, quartz, and granite pebbles, interbedded with fine-grained sandstones and laminated shales.	Coarse-grained lithic sandstone	

Sample	Stratigraphic-Unit	Outcrop description	Sample lithology	Description hand specimen
4Apr18-5A	Encanto Formation	Section with gray shales with pencil foliation and parallel lamination with very fine/grained calcareous sandstone. The section is drastically interrupted by a massive coarse to medium/grained sandstone, 1.5 m thick, tabular, with a sharp base. The sandstone bed is overlain by laminated calcareous grey shales.	vf-f-grained calcareous sandstone	Very fine-grained sandstone.
2Apr18-2B	Depósito Formation	Greenish, coarse-grained sandstones interbedded with fine-grained sandstones and siliceous shales, conglomerates, sandstones, and shales. The conglomerates are made of rhyolites. The outcrop is affected by a fault bend fold.	Coarse to vf-grained lithic sandstone	
4Apr18-3B	Nanchital Shale	Gray laminated shales interbedded with sandstones in tabular beds.	Coarse-grained lithic arkose	Coarse-grained sandstone, with Quartz (70%), Feldspar, green lithics, potassium feldspar, white micas.

a)



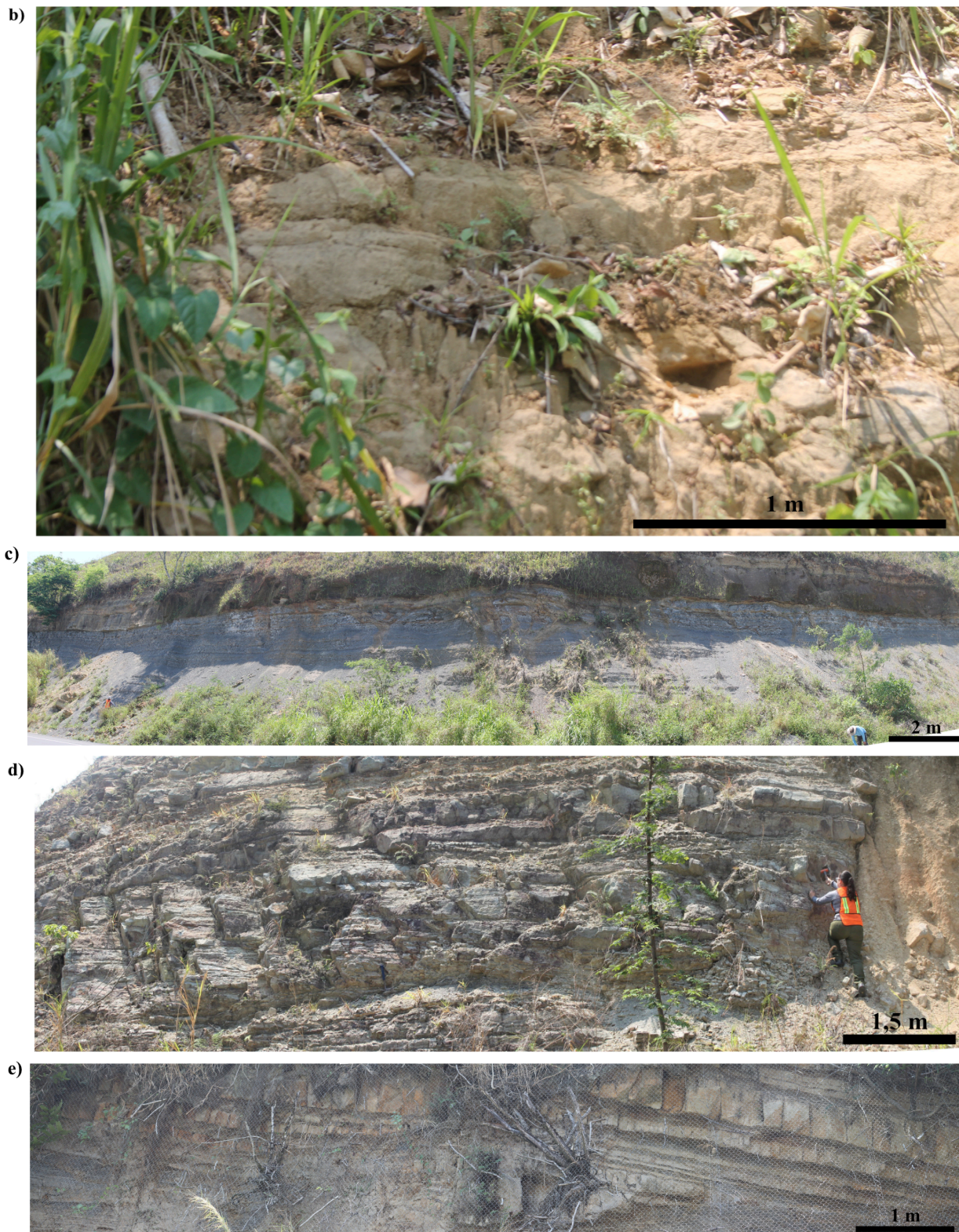


Figure 11. Photographs of the outcrops where the samples were taken from Comalcalco and Macuspana basins, 2018: a) 6Apr18-3B sample from Amate Formation of Macuspana basin: medium-grained lithic sandstone; b) 2Apr18-5B sample from Filisola Formation of Comalcalco basin: massive coarse-grained sandstones, pebbly sandstones, and shales; c) 4Apr18-5A sample from Encanto Formation of Comalcalco basin: sandstone; d) 2Apr18-2B sample from Depósito Formation of Comalcalco basin: lithic sandstone; e) 4Apr18-3B sample from Nanchital Shale of Comalcalco basin: Lithic arkose. [Photographs by María Isabell Sierra].

4. METHODOLOGY

Sample preparation

Heavy mineral research requires separation process from their host rock and this can be achieved by the disaggregation of the rock and mineral separation (Mange & Maurer, 2012). The samples were disaggregated by trituration and passed through a 125 µm diameter sieve. The sieved fraction was portioned using the quartering method. The resulting quarter portion was washed to clean out the great amount of clay present in the samples.

In mineral separation procedure, using the heavy liquids method is more efficient than panning. However, we did not have access to those liquids to perform the separation. Thus, a pan was used to separate the heavy portion of minerals from the light ones (see Figure 12a). The results show that in panning method several light minerals such as quartz, K-feldspars, plagioclase were not discharged; thus, the panning approach should be used by caution. The light minerals were taken off by manual picking up. It was possible to obtain concentrates of heavy minerals such as amphibole, apatite, chloritoid, chlorite, chromium spinel, epidote, garnet, ilmenite, rutile, staurolite, titanite, and zircon.

In the heavy portion, the ferromagnetic minerals were separated using a magnet (catching mostly magnetite grains) and the paramagnetic and the diamagnetic minerals were separated in groups by applying different electrical currents using a Frantz separator (see Figure 12b). It was expected that using the Frantz, each paramagnetic fraction will contain specifically certain heavy minerals or at least a really high proportion of them according to the electric current they were subjected to, but it was not possible to separate them in groups using this method. However, we could concentrate opaque minerals in the lowest amperes section and minerals such as zircons and apatites in the non-magnetic portion.

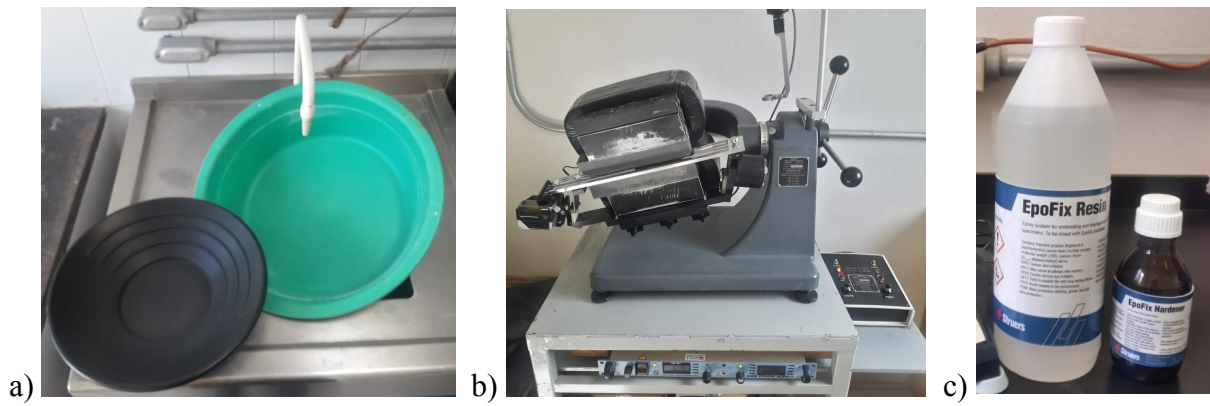


Figure 12. Photographs of the techniques used for mineral separation: a) Pan; b) Frantz separator. c) EpoFix used to mount the samples.

After the separation process, samples were mounted in resin (8g of EpoFix resin and 1.2g of hardener, Figure 12c), each one containing two samples (Figure 13). To prepare samples for optical microscopic studies, the surface of the mounts was polished.

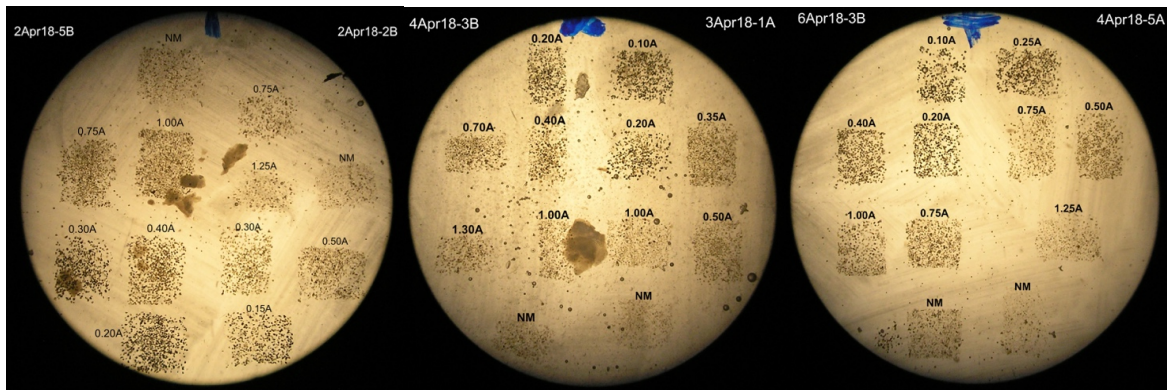


Figure 13. Photographs of the samples on the EpoFix mounts; each side, left and right, contains one sample. In the upper part of each group it is written the applied intensity of current.

Petrographic analysis

Conventional petrography is the primary technique to determine the mineralogical composition and textural features of the samples. Although the recent tendency is to apply more reliable and sophisticated instruments, the examination by the petrographic microscope remains necessary (Garzanti, 2016). Therefore, a petrographic analysis of the grains was performed in order to

describe and determine which heavy mineral grains are present in the samples. The Olympus BX53 microscope was used in both reflected- and transmitted-light modes at the School of Earth, Energy and Environmental Sciences of Yachay Tech University. One important thing to consider is that the birefringence color was not possible to determine for all minerals because there were analyzed polished grains, not in a thin section; thus, the grains are thick which may alter the color. Doubly polished process was not made to avoid take off some minerals. For this reason, in the petrographic analysis, I took more into account other optical properties such as relief, or habit.

SEM analysis

The grains were analyzed by using a scanning electron microscope (SEM) of the Nanomaterials Characterization Laboratory at the Universidad de las Fuerzas Armadas ESPE, Ecuador. Prior to analysis, the mounted pucks were covered by gold, using a Sputter Coating Quorum Q105R gold evaporator producing a gold cover layer of an approximate thickness of 20 nm. Then, the grains were analyzed using a SEM instrumentation (TESCAN model MIRA 3). This microscope shows the morphology of minerals and the elemental compositions determined by the EDS (Energy-dispersive X-ray spectroscopy). The EDS was performed using a Bruker X-Flash 6j30 detector, while the observations were made with the backscattered Electron (BSE) detector performed at 25.00 KV. Each peak on the resulted EDS spectra represents a qualitative composition of major elements on grains (usually elemental concentrations greater than 1% are displayed). One important thing to consider is that in some EDS spectra there are C picks, this does not mean C is one of the principal element represented in the spectra, this probably was caused by the presence of CO₂ in the environment before to put the mount sample in the SEM machine, leaving some carbon particles impregnated on the mount's surface.

Among the heavy mineral chemical analysis, garnet is selected for classifying them into different groups according their chemical composition. This is because garnet can be expressed as percentages of its six end-members. The major elements of various garnet gains (9) obtained by SEM analysis and the calculation of the percentage of each garnet end-member was done following the steps described by Brady & Perkins (2017): 1) The obtained percentage of each

element was divided by its molar weight to know the number of moles of the element; 2) Form oxides and calculate the percentage of each oxide in the mineral; 3) Divide the weight percentage of each oxide by the formula weight of that oxide; 4) Multiply the resulting "mole number" of each oxide by the number of oxygens in the oxide formula; 5) Multiply the resulting "oxygen number" of each oxide by a normalization constant (equal to the number of oxygens in the desired formula divided by the sum of the "oxygen numbers"); and 6) Multiply the "normalized oxygen numbers" of each oxide by the number of cations per oxygen in the oxide formula.

5. RESULTS

Heavy mineral suites

The found heavy minerals in this study are Ti-bearing amphibole, apatite, chlorite, chloritoid, chromian spinel, epidote garnet, ilmenite, rutile, staurolite, titanite, and zircon. Figure 14 shows the percentage of occurrence of those minerals in relation to the overall amount of heavy minerals in each sample associated to the Formation they belong.

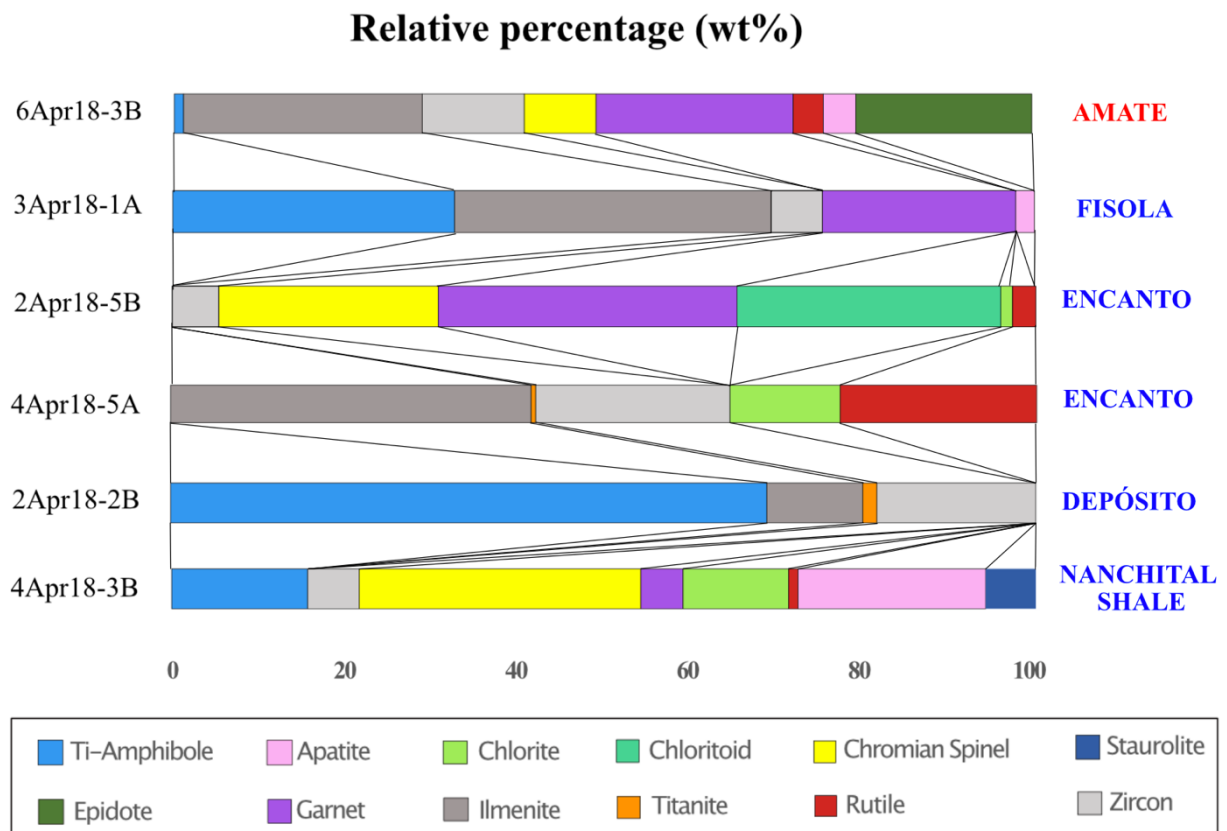


Figure 14. Relative percentages of heavy minerals found in the analyzed samples. To the right there are the corresponding formation to which samples were taken. Formations are ordered following the stratigraphy; the red text belongs to the Macuspana basin, and the blue text to the Comalcalco basin.

Petrographic results

Twelve different heavy minerals were identified by petrographic studies in the examined samples, including Ti-bearing amphibole, apatite, chlorite, chloritoid, chromian spinel, epidote,

garnet, ilmenite, rutile, staurolite, titanite, and zircon. The detailed description of the aforementioned heavy minerals is followed.

The *Ti-bearing amphibole* grains are present in 6Apr183B (Amate Formation, upper Miocene), 3Apr18-1A (Filisola Formation, early upper Miocene), 4Apr18-3B (Nanchital Shale, early lower Miocene), and 2Apr18-2B (Depósito Formation, lower Miocene) samples (Figures 15, 16, 19, and 20 respectively), reaching almost 70% modal of the heavy mineral suite in the Depósito Formation sample. The tabular habit of amphibole assists to identify them easily. They are translucent and their typical color is greenish-brown (Figure 19), brown (Figures 16, 19, and 20) or blueish-green (Figure 15), and all amphibole are pleochroic. In some of them, determination of the optic sign was possible, being biaxial negative.

The *Apatite* grains were found in 6Apr183B (Amate Formation, upper Miocene), 4Apr18-3B (Nanchital Shale, early lower Miocene), and 3Apr181A (Filisola Formation, early upper Miocene) samples, ranging from 2% to 21% modal of abundance of the heavy mineral suite. They were identified based on their high relief. Some of them are transparent and others have brown color (Figure 16).

Chlorite is present in 4Apr18-5A (Encanto Formation, middle Miocene), 4Apr18-3B (Nanchital Shale, early lower Miocene), and 2Apr18-5B (Encanto Formation, middle Miocene) samples, ranging from 1 to almost 12% modal of the heavy mineral suite. The chlorite grains are greenish-blue, brown, or light green (Figures 17, 18, and 20 respectively), the light green ones were easier to identify because of their color and the mica-like habit. Furthermore, they present weak pleochroism. Also, they have a biaxial optic sign.

The *Chloritoid* grains were found in the 2Apr18-5B sample (Encanto Formation, middle Miocene) (Figure 17), representing 30% modal of the heavy mineral suite. They are translucent, yellow in color, and pleochroic. These grains were not easy to identify by microscopic studies, therefore, SEM-EDS performed.

Chromian spinel was found in 6Apr183B (Amate Formation, upper Miocene), 4Apr18-3B (Nanchital Shale, early lower Miocene), and 2Apr18-2B (Depósito Formation, lower Miocene) samples, ranging from 8 to 32% modal of the heavy mineral suite. This is the most abundant heavy mineral in the 4Apr18-3B sample. Some chromian spinel grains show the opaque mineral

feature (Figures 17 and 20) and the other ones are translucent dark brown (Figures 15, 17, and 20) with medium-high relief. SEM-EDS analysis identified the optically opaque grains.

Epidote, up to 20% modal of the heavy mineral suite was identified in 6Apr183B sample (Amate Formation, upper Miocene). Epidote grains are translucent of light green color. They are weakly pleochroic and present a high relief (Figure 15).

Garnet was found in 6Apr183B (Amate Formation, upper Miocene), 4Apr18-3B (Nanchital Shale, early lower Miocene), 3Apr18-1A (Filisola Formation, early upper Miocene), and 2Apr18-5B (Encanto Formation, middle Miocene) samples, ranging from 4 to 34% modal of the heavy mineral suite. In the Encanto Formation sample, garnet is the most abundant heavy mineral up to 34.6%. Garnet grains are translucent, having high relief. Some of them are rounded (Figures 15, 16, and 17), whereas others have an irregular shape (Figures 15, 16, and 20). Most of them have a light pink color (Figures 15, 16, 17, 20), and few are light green and light orange (Figure 15), or transparent (Figure 16). In some of the light pink, it was possible to determine the optic sign, having a biaxial negative one.

Ilmenite was found in 6Apr183B (Amate Formation, upper Miocene), 4Apr18-5A (Encanto Formation, middle Miocene), 2Apr18-2B (Depósito Formation, lower Miocene), and 3Apr181A (Filisola Formation, early upper Miocene) samples, ranging from 10 to 41% modal of the heavy minerals suite, and is the most abundant heavy mineral in the Filisola Formation sample. Ilmenite grains are all opaque and present an irregular (Figure 16 and 18) or sub-rounded shape (Figure 15 and 19). SEM-EDS analysis helped to identify them.

Rutile was found in 6Apr183B (Amate Formation, upper Miocene), 4Apr18-5A (Encanto Formation, middle Miocene), 4Apr18-3B (Nanchital Shale, early lower Miocene), and 2Apr18-5B (Encanto Formation) samples, ranging from 1 to 22% modal of the heavy minerals suite. Some rutile grains are translucent, showing reddish-brown (Figures 15, 17, and 18), brown (Figure 15) or brownish-yellow color (Figure 18), and the other ones are opaque (Figure 20). The translucent ones were easy to identify based on their color and the high relief; for some of them based on their extinction angle. Furthermore, they are weakly pleochroic and have parallel extinction. There are elongated-shape rutile grains (Figure 15) while others are more equant, being the last ones, sub-angular grains (Figure 15, 17, 18, and 20), may be caused by abrasion during its transport toward the basins.

Staurolite was found only in the 4Apr18-3B sample (Nanchital Shale, early lower Miocene), being the 6% modal of the heavy mineral suite. *Staurolite* grains (Figure 20) are translucent, gray or bright light yellow in color, pleochroic, and present irregular shapes. Both varieties present high relief. Based on the color of the yellow one and their relief they were selected as *staurolite* grains but it was necessary to look their SEM-EDS spectra of them to confirm; while the gray ones were identified by SEM-EDS spectra.

The small amount of *Titanite* in 4Apr18-5A (Encanto Formation, middle Miocene) and 2Apr18-2B (Depósito Formation, lower Miocene) samples were identified, having less than 2% modal of the heavy mineral suite. *Titanite* grains are translucent and weakly pleochroic. They were classified into two different groups based on their color and shape. One group is light pink in color and has an almost perfect crystalline shape (Figure 18), being obvious their monoclinic crystal system, and due to its high relief, they were easily identified. The second group is light yellow, with an irregular shape, and presents a high relief too (Figure 19).

High number of *Zircons* were found in all samples: 6Apr183B (Amate Formation, upper Miocene), 4Apr18-5A and 2Apr18-5B (Encanto Formation, middle Miocene), 3Apr181A (Filisola Formation, early upper Miocene), 2Apr18-2B (Depósito Formation, lower Miocene), and 4Apr18-3B (Nanchital Shale, early lower Miocene) samples, ranging from 5 to 22% modal of the heavy mineral suite. *Zircon* grains were the easier grains to identify during the petrographic analysis because of their really high relief and their obvious tetragonal crystal system. Most of them are transparent (Figure 15, 16, 17, 18, and 20) and few have light pink color (Figure 19). Most grains are close to equant shape, anhedral-rounded (Figures 15, 17, 18, 19, 20) or euhedral (Figure 16), and the other ones are elongated and euhedral (Figure 16).

The identified minerals and their respective samples studied in this job are shown in Table 2. Also, images of aforementioned heavy minerals are shown in Figures 15-20. The detailed petrographic description of those minerals is presented in Appendix 1.

Table 2. Minerals found by Petrographic analysis. The range of percentage of each mineral in the overall heavy mineral suite is represented by the following colors: green, yellow, orange, and blue for 0-10%, 10-20%, 20-40%, and 40-70% respectively. **Legend:** Amp: amphibole; Ap: Apatite; Chl: Chlorite; Chr: Chromian spinel; Cld: Chloritoid; Ep: Epidote; Gt: Garnet; Ilm: Ilmenite; Rt: Rutile; St: Staurolite; Ttn: Titanite; Zrn: Zircon.

Stratigraphic Unit	Sample	Amp	Ap	Chl	Chr	Cld	Ep	Gt	Ilm	Rt	St	Ttn	Zrn
Amate Fm.	6Apr18-3B	x	x		x		x	x	x	x			x
Filisola Fm.	3Apr18-1A	x	x					x	x				x
Encanto Fm.	2Apr18-5B			x	x	x		x		x			x
Encanto Fm.	4Apr18-5A			x					x	x		x	x
Depósito Fm.	2Apr18-2B	x							x			x	x
Nanchital Shale	4Apr18-3B	x	x	x	x			x		x	x		x

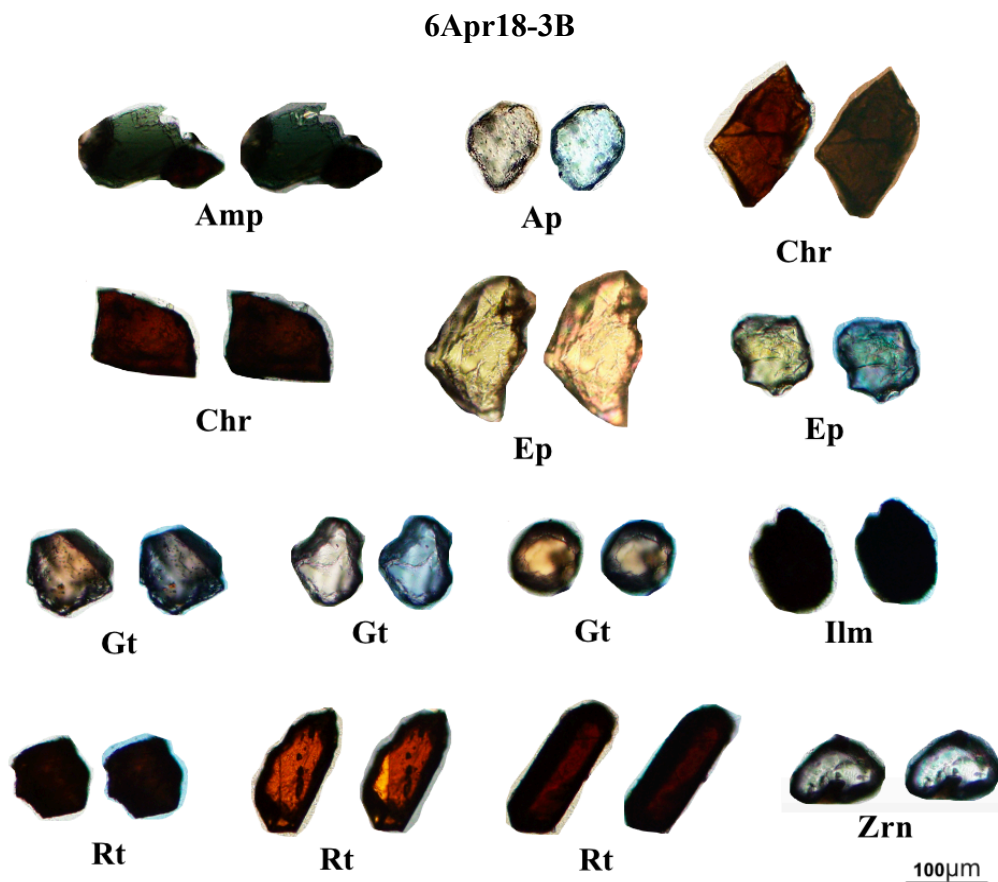


Figure 15. Heavy minerals found in 6Apr18-3B sample (Amate Formation). The left side is an image taken under plane polarized light, the right one is taken under cross polarized light. Legend: Amp: Amphibole; Ap: Apatite; Chr: Chromian spinel; Ep: Epidote; Gt: Garnet; Ilm: Ilmenite; Rt: Rutile; Zrn: Zircon.

3Apr18-1A

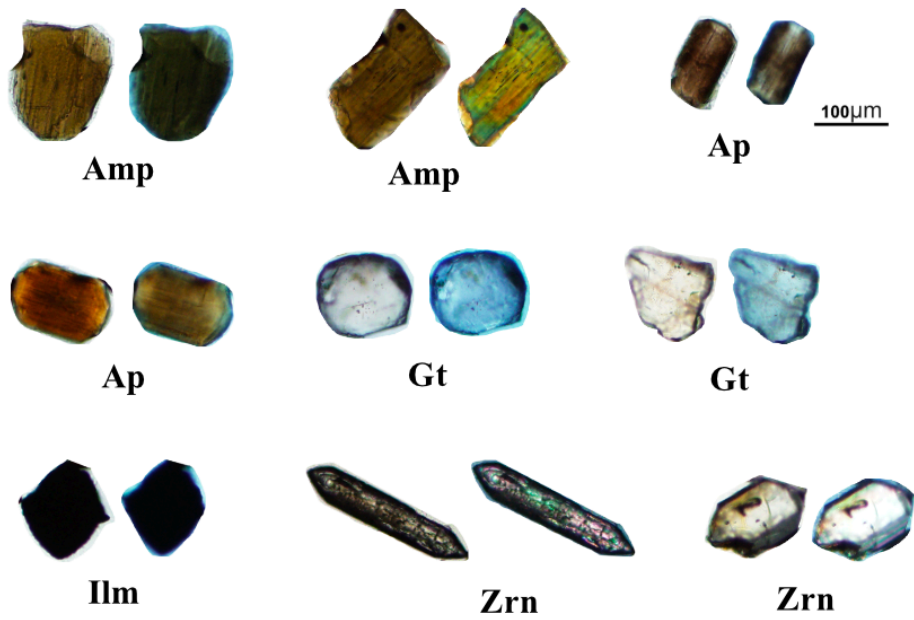


Figure 16. Heavy minerals found in 3Apr18-1A sample (Filisola Formation). The left side is an image taken under plane polarized light, the right one is taken under cross polarized light. Legend: Amp: amphibole; Ap: Apatite; Gt: Garnet; Ilm: Ilmenite; Zrn: Zircon.

2Apr18-5B

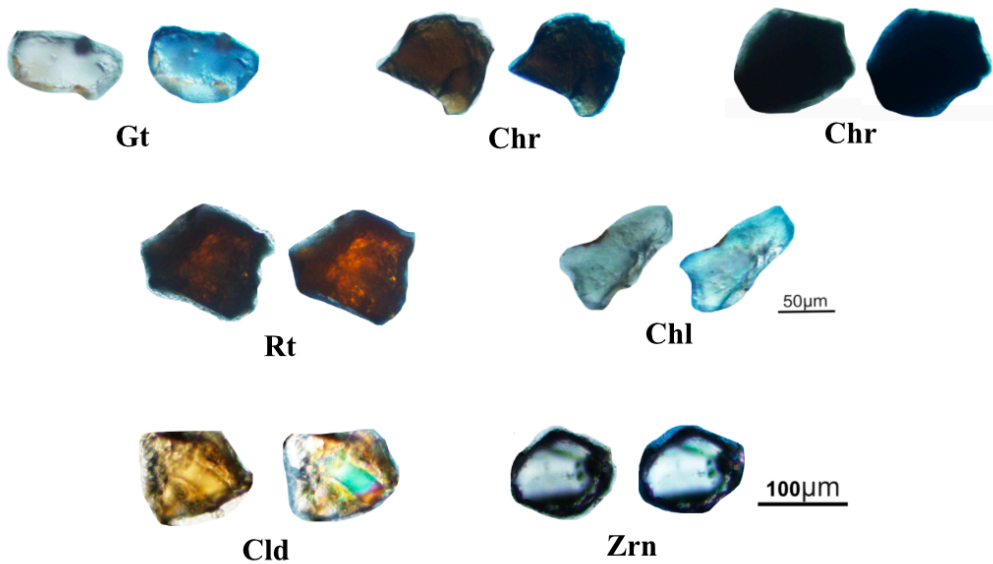


Figure 17. Heavy minerals found in 2Apr18-5B sample (Encanto Formation). The left side is an image taken under plane polarized light, the right one is taken under cross polarized light. Legend: Chr: Chromian spinel; Chl: Chlorite; Cld: Chloritoid; Gt: Garnet; Rt: Rutile; Zrn: Zircon.

4Apr18-5A

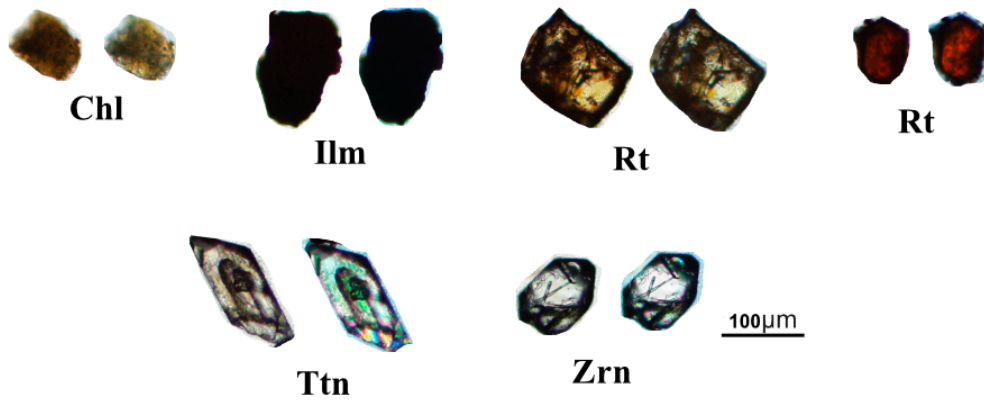


Figure 18. Heavy minerals found in 4Apr18-5A sample (Encanto Formation). The left side is an image taken under plane polarized light, the right one is taken under cross polarized light. Legend: Chl: Chlorite; Ilm: Ilmenite; Rt: Rutile; Ttn: Titanite; Zrn: Zircon.

2Apr18-2B

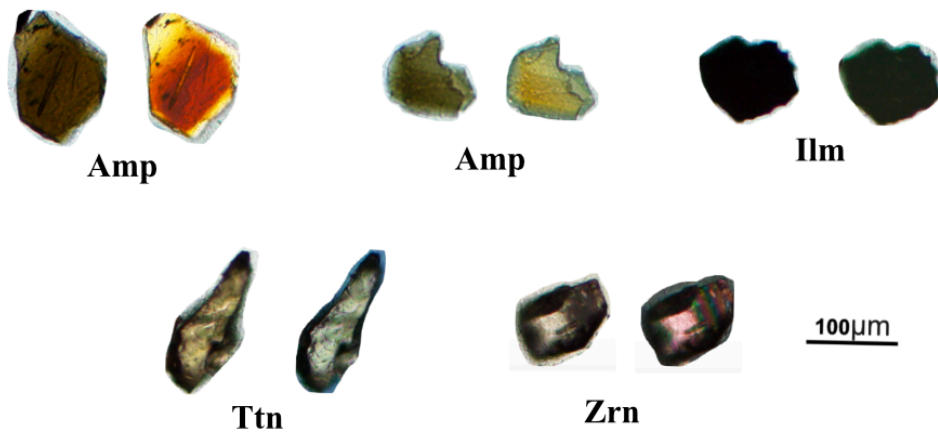


Figure 19. Heavy minerals found in 2Apr18-2B sample (Depósito Formation). The left side is a photograph taken under plane polarized light, the right one is taken under cross polarized light. Legend: Amp: amphibole; Ilm: Ilmenite; Ttn: Titanite; Zrn: Zircon.

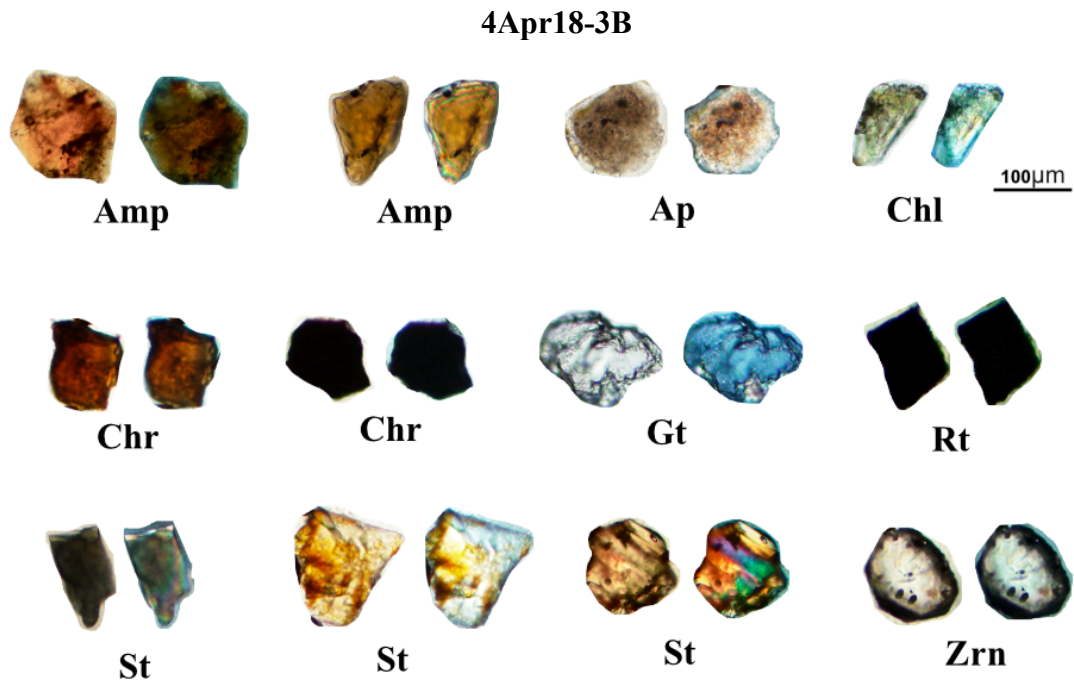


Figure 20. Heavy minerals found in 4Apr18-3B sample (Nanchital Shale). The left side is an image taken under plane polarized light, the right one is taken under cross polarized light. Legend: Amp: amphibole; Chl: Chlorite; Chr: Chromian spinel; Gt: Garnet; Rt: Rutile; St: Staurolite; Zrn: Zircon.

SEM-EDS results

The result of SEM-EDS analysis on the heavy mineral of interest is presented in this section (see Figures 21-32).

Ti-bearing amphibole

The Ti-bearing amphibole can be recognized by the EDS spectrum main peaks of Si, O, Ca, Al, Mg, Fe, Ti, and Na as suggested by Reed (2005) (see Figure 21). This mineral was found in four samples: 6Apr18-3B, 3Apr18-1A, 2Apr18-2B, 4Apr18-3B (see Figures 15, 16, 19, and 20 respectively in the petrographic results section), from the lower Miocene to the early upper Miocene.

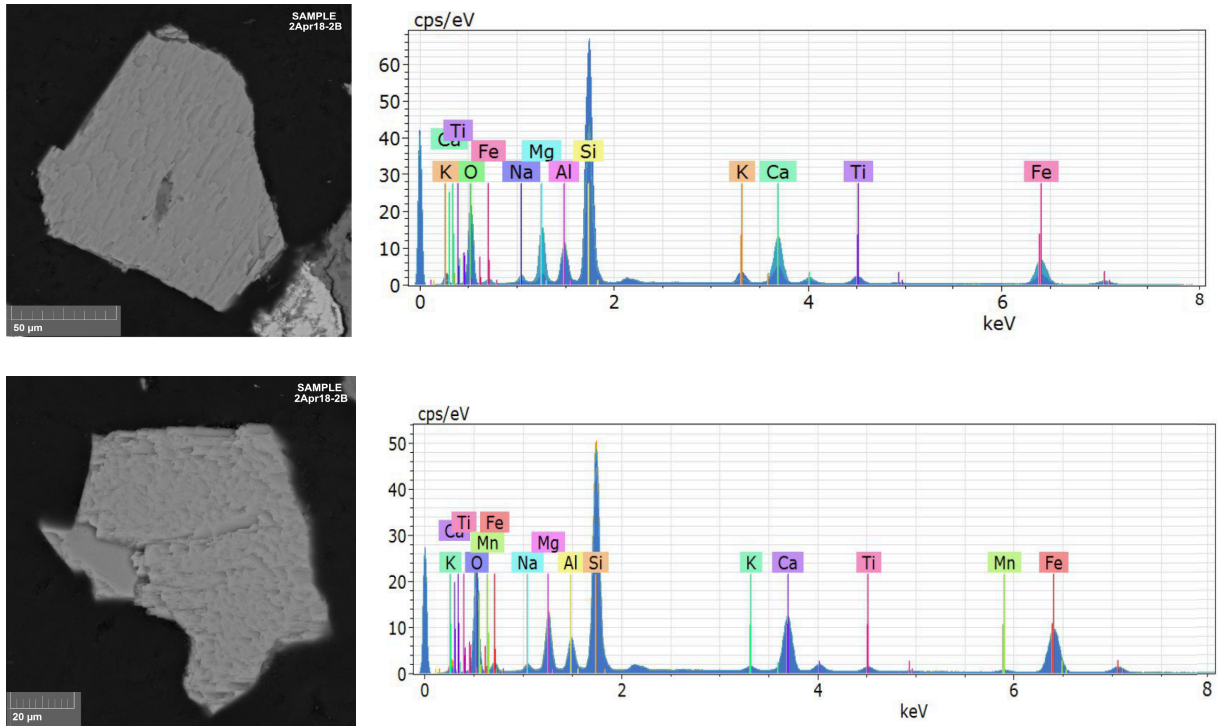
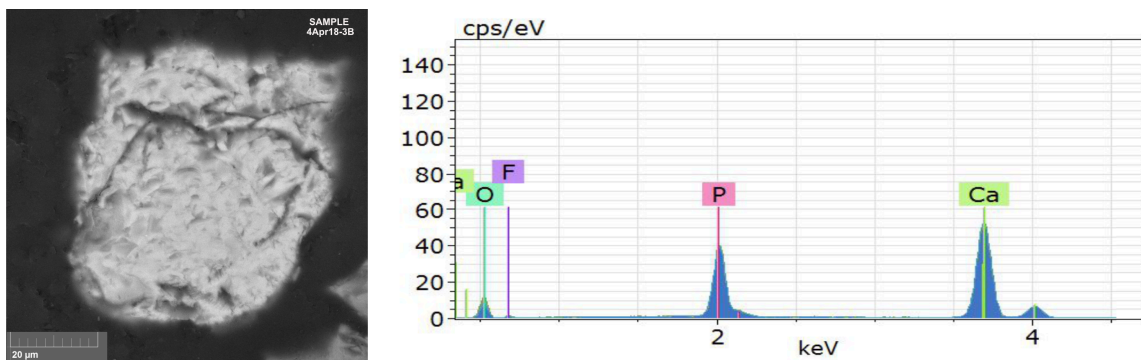


Figure 21. SEM photos and EDS spectra of Ti-bearing amphibole.

Apatite

The EDS spectra of apatite grains (see Figure 22) show Ca, P, O as main peaks accompanied by the presence of F and/or Cl picks (Reed, 2005). The same features have been seen in the studied mineral of three samples: 6Apr18-3B, 3Apr18-1A, and 4Apr18-3B (see Figures 15, 16, and 20 respectively in the petrographic results section), more abundant in the lower Miocene sediments (4Apr18-3B of Nanchital Shale).



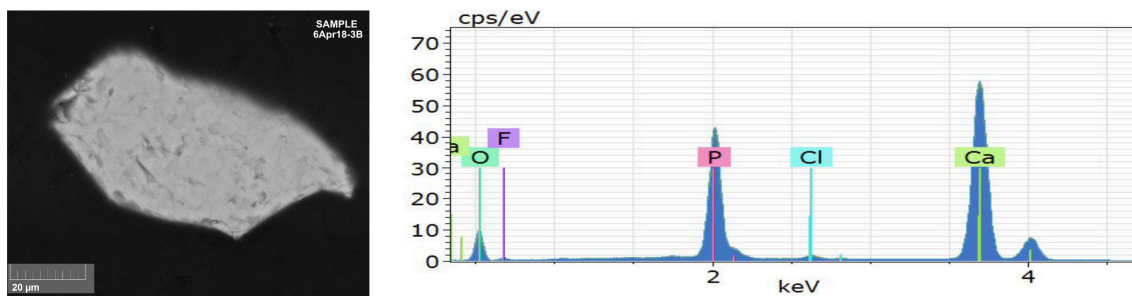


Figure 22. SEM photos and their EDS spectra of Apatite.

Chlorite

Chlorite from 2Apr18-5B, 4Apr18-5A, 4Apr18-3B (see Figures 17, 18, and 20 respectively in the petrographic results section) samples demonstrated EDS spectrum main peaks of O, Si, Al, Mg, Fe (Reed, 2005) (see Figure 23). This mineral is more abundant during the early lower (4Apr18-3B of Nanchital Shale) to middle Miocene (4Apr18-3B of Encanto Formation).

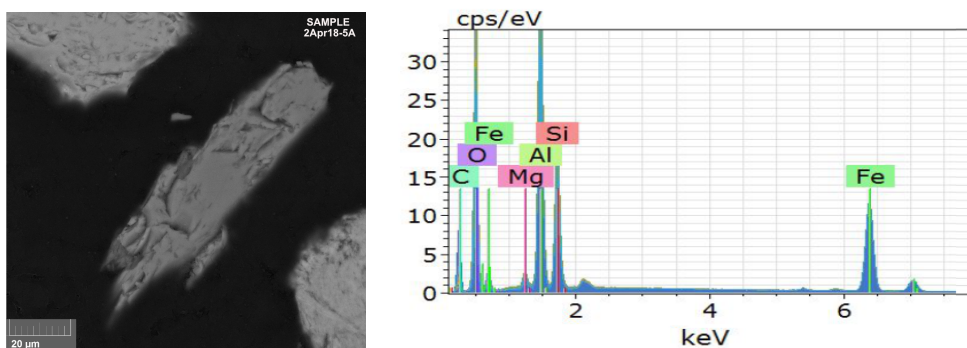


Figure 23. SEM photo and EDS spectrum of Chlorite.

Chloritoid

The SEM-EDS analysis of chloritoid in sample 2Apr18-5B (see Figure 17 in the petrographic results section) from Encanto Formation (middle Miocene) show elevated spectra of O, Al, Si, and Fe (Reed, 2005) (see Figure 24). The anomalous Ca spectrum most likely is related to carbonate mineral contamination, showing a peak for C as well.

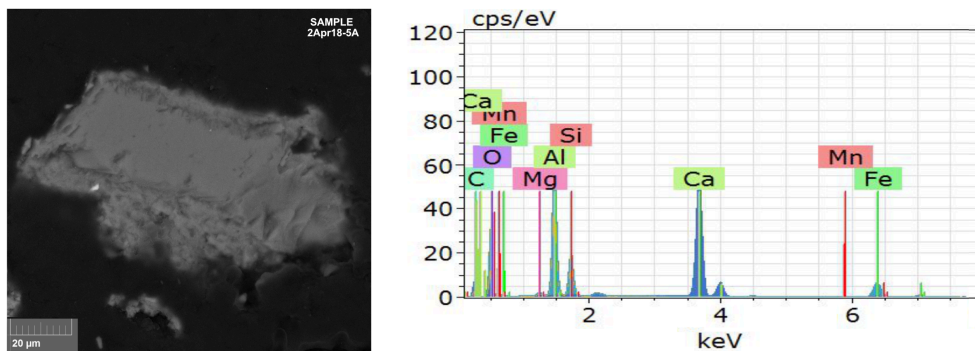


Figure 24. SEM photos of Chloritoid and its EDS spectrum.

Chromian spinel

Chromian spinel can be easily identified by showing a peak of Cr in the SEM-EDS spectra. Chromian spinel has Mg, Fe, Cr, Al, and O elements in their chemical composition (Lee, 1999), which is represented in the analyzed grains (see Figure 25). This mineral was found in three samples: 6Apr18-3B, 2Apr18-5B, 4Apr18-3B (see Figures 15, 17, and 20 respectively in the petrographic results section), from early lower Miocene to upper Miocene.

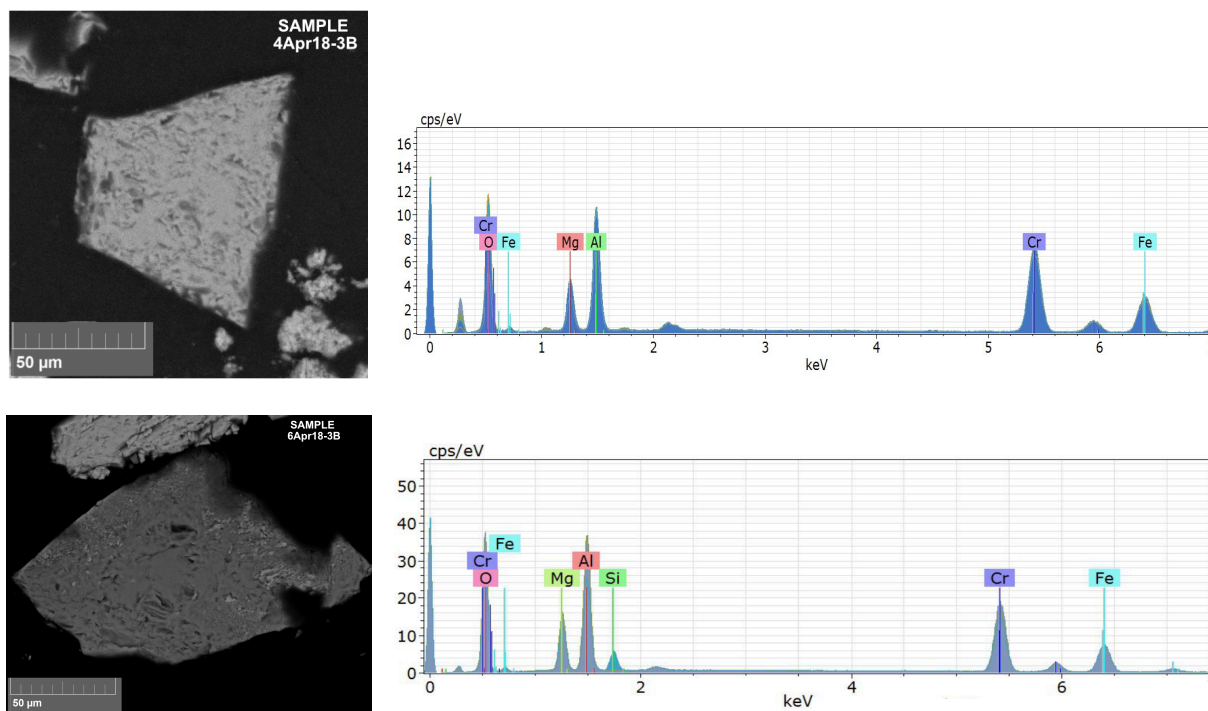


Figure 25. SEM photos and EDS spectra of Chromian spinel.

Epidote

The EDS main peaks in epidote only within 6Apr18-3B sample (see Figure 15 in the petrographic results section) of Amate Formation (upper Miocene) is identified for Si, O, Al, Ca elements, followed by Fe element (see Figure 26).

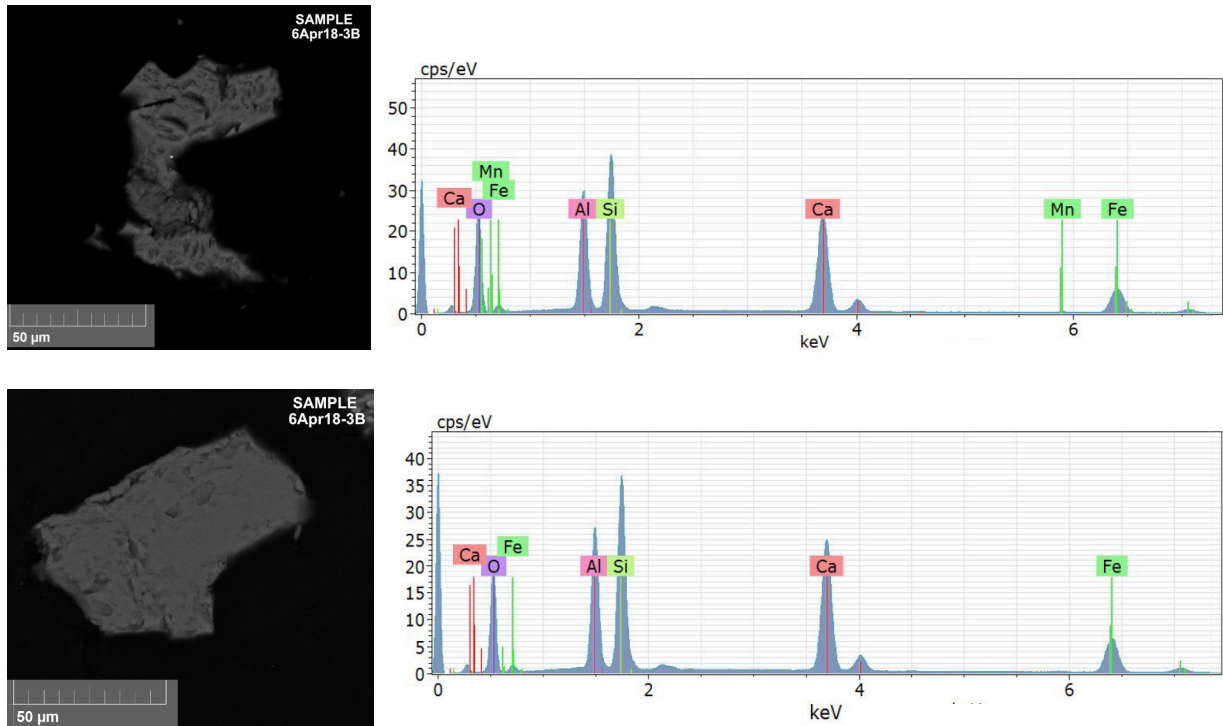


Figure 26. SEM photos and EDS spectra of Epidote.

Garnet

The EDS spectra of garnet (see Figure 27) always show Si, O, Al elements as peaks, and Ca, Cr, Fe, Mg, Mn elements (Reed, 2005). In the analyzed garnets, the Cr element was absent. This mineral was found in four samples: 6Apr18-3B, 3Apr18-1A, 2Apr18-5B, and 4Apr18-3B (see Figures 15, 16, 17, and 20 respectively in the petrographic results section), more abundant in middle to upper Miocene sediments.

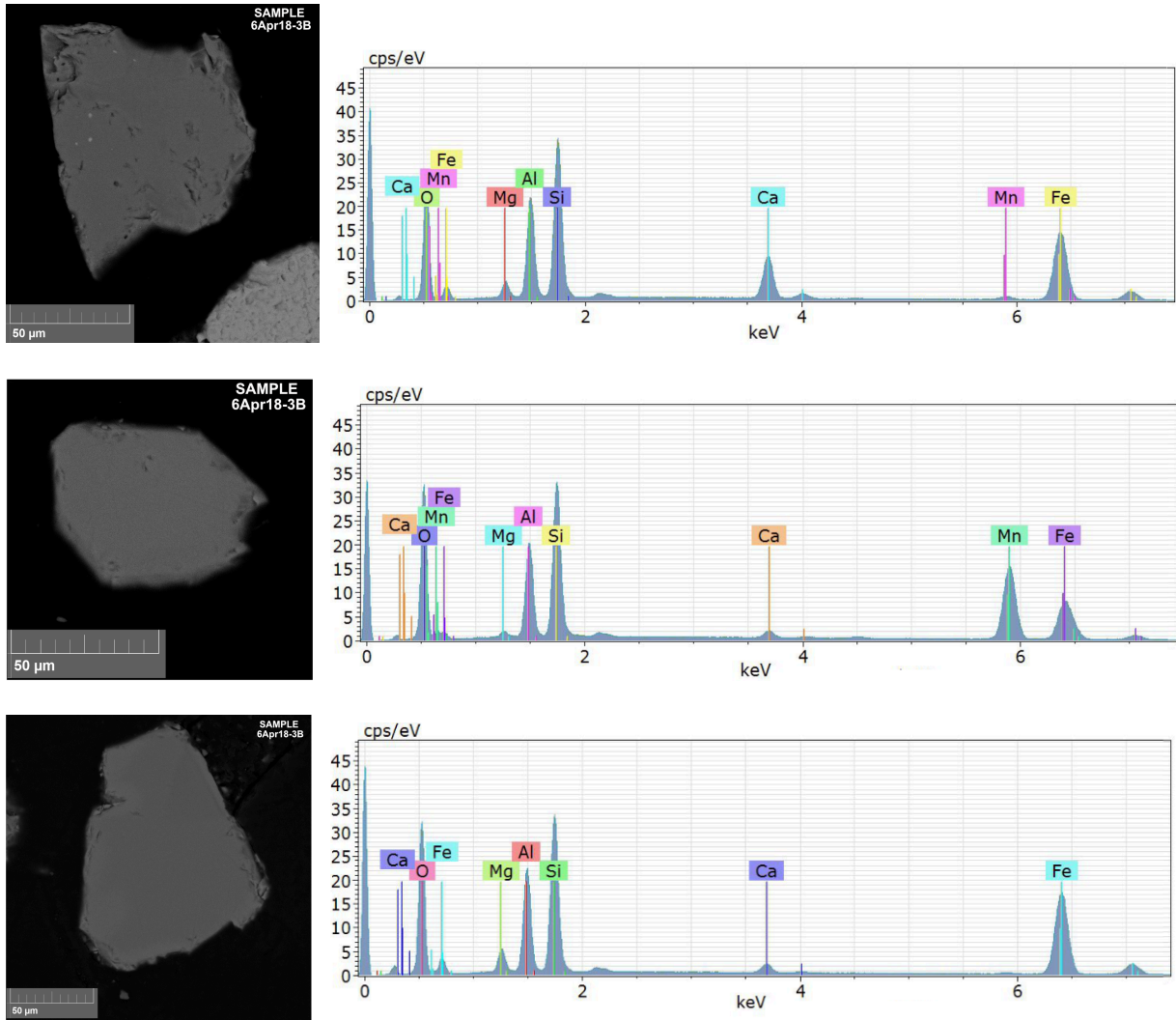


Figure 27. SEM photos and EDS spectra of Garnet.

Ilmenite

The EDS spectra of ilmenite (see Figure 28) show Ti, Fe, and O elements as main peaks (Reed, 2005). This mineral was found in four samples: 6Apr183B, 3Apr181A, 4Apr18-5A, and 2Apr18-2B (see Figures 15, 16, 18, and 19 respectively in the petrographic results section), mainly in middle to upper Miocene sediments (6Apr183B and 3Apr181A of Amate and Filisola Formations respectively).

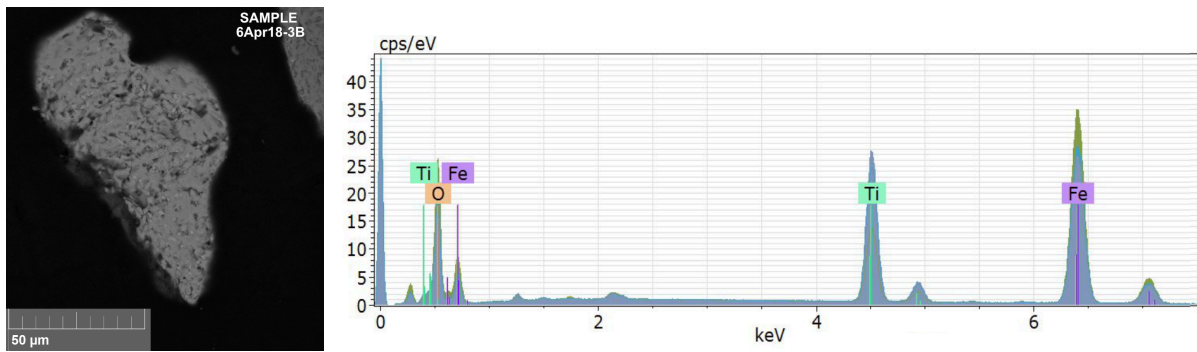


Figure 28. SEM photo and EDS spectrum of Ilmenite.

Rutile

The EDS spectra of rutile (see Figure 29) always show Ti and O elements as peaks (Reed, 2005). This mineral was found into four samples: 6Apr18-3B, 2Apr18-5B, 4Apr18-5A, and 4Apr18-3B (see Figures 15, 17, 18, and 20 respectively in the petrographic results section), but more abundant during the middle Miocene in sample 4Apr18-5A of Encanto Formation.

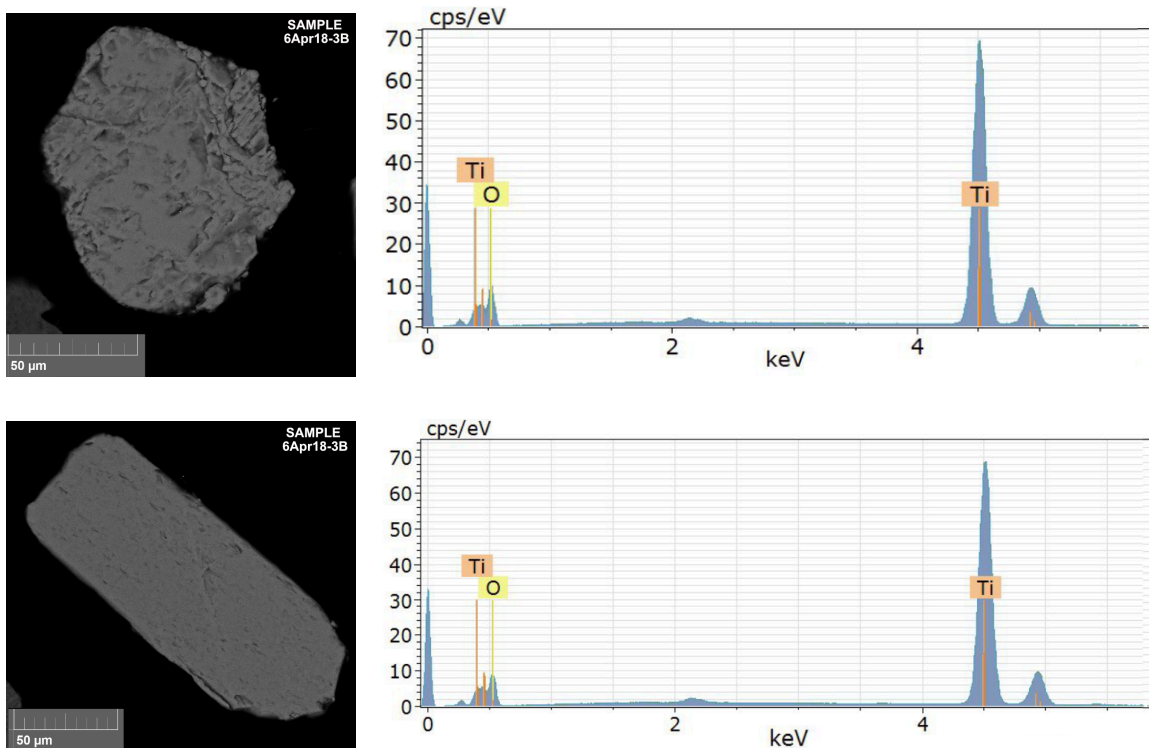


Figure 29. SEM photos and EDS spectra of Rutile.

Staurolite

In the EDS spectra of staurolite (see Figure 30), the main peak is Al, followed by O, Si, Fe, and Mg elements (Reed, 2005). This mineral was found only in one sample: 4Apr18-3B (see Figure 20 in the petrographic results section) from the early lower Miocene (Nanchital Shale).

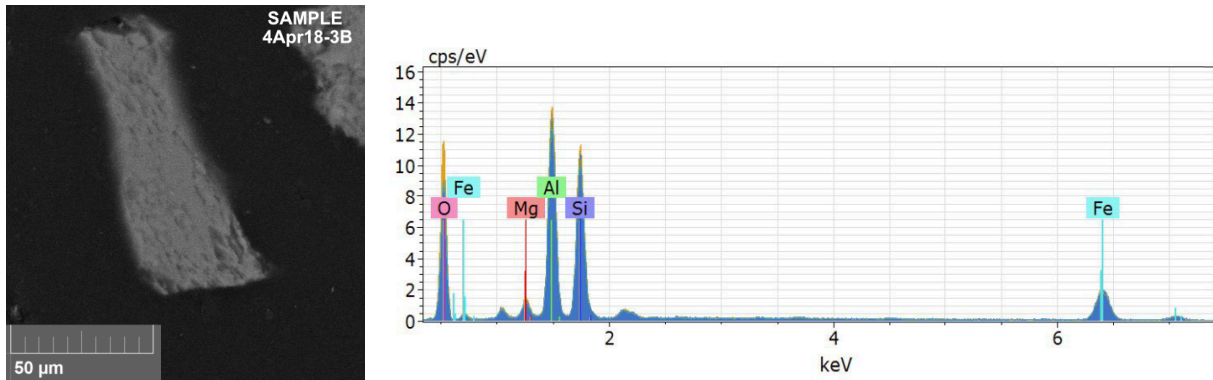


Figure 30. SEM photo and EDS spectrum of Staurolite.

Titanite

Titanite can be recognized because the EDS spectrum shows Si, Ca, Ti, O as main peaks (Reed, 2005) (see Figure 31). This mineral was found with low abundance in two samples: 2Apr18-2B and 4Apr18-5A of Depósito and Encanto Formation samples (see Figures 18 and 19 respectively in the petrographic results section) from the late lower – middle Miocene respectively.

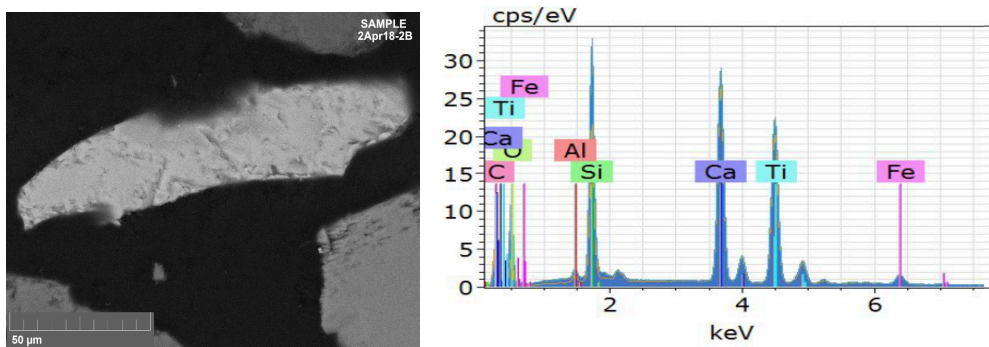


Figure 31. SEM photo and EDS spectrum of Titanite.

Zircon

Zircon grains can be easily identified by showing Zr, Si, and O elements as main peaks (Reed, 2005) (see Figure 32). This mineral was found in all samples: 6Apr183B, 3Apr18-1A, 2Apr18-5B, 4Apr18-5A, 2Apr18-2B, 4Apr18-3B (see Figures 15, 16, 17, 18, 19, and 20 respectively in the petrographic results section) from early lower – to upper Miocene sediments.

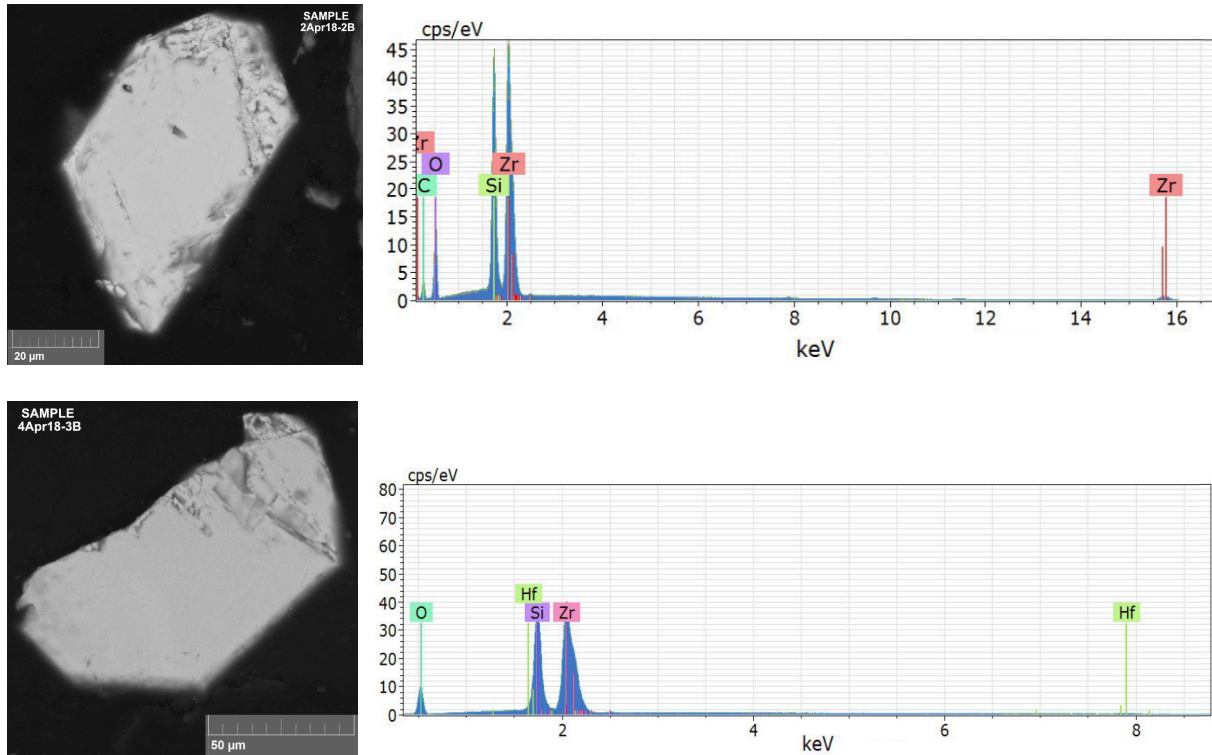


Figure 32. SEM photos and EDS spectra of Zircon.

Garnet chemistry

The garnet grains studied do not contain substantial amounts of Cr. The garnet classification was done based on chemical composition of five possible end-members (pyrope, almandine, spessartine, grossular, and andradite). Table 3 shows the composition in oxides of the detrital garnets and Table 4 presents the percentage of end-members of garnet grains.

Table 3. Composition of garnets from SEM-EDS analysis (in wt. % of oxides).

Group	Sample	SiO ₂	Al ₂ O ₃	Fe ₂ O ₃	FeO	MnO	MgO	CaO
G3	2Apr18-5B	33,78	15,22	16,81	18,29	9,60	4,30	3,67
G3	3Apr18-1A	33,46	14,42	16,12	23,99	9,54	2,24	1,84
G3	3Apr18-1A	36,01	16,38	8,00	25,05	10,50	2,27	2,59
G3	3Apr18-1A	32,67	13,37	20,93	10,41	14,90	1,96	7,86
G3	4Apr18-3B	34,04	14,96	15,84	17,49	10,14	2,50	6,63
G2	6Apr18-3B	33,96	14,85	20,97	16,90	2,97	9,47	2,98
G2	6Apr18-3B	33,11	13,95	23,83	11,68	1,19	5,65	12,97
G4	6Apr18-3B	34,87	14,54	13,15	4,37	29,74	2,48	2,17
G1	6Apr18-3B	34,30	15,10	19,17	21,72	0,00	8,79	2,84

Table 4. Relative abundance of garnet end-members (in Mol%).

Group	Sample	Pyrope (%)	Almandine (%)	Spessartine (%)	Grossular (%)	Andradite (%)
		Mg ₃ Al ₂ (SiO ₄) ₃	Fe ₃ Al ₂ (SiO ₄) ₃	Mn ₃ Al ₂ (SiO ₄) ₃	Ca ₃ Al ₂ (SiO ₄) ₃	Ca ₃ Fe ₂ (SiO ₄) ₃
G3	2Apr18-5B	19,00	45,29	24,08	6,82	4,81
G3	3Apr18-1A	9,98	59,96	24,15	3,45	2,46
G3	3Apr18-1A	9,41	58,18	24,7	5,88	1,83
G3	3Apr18-1A	8,93	26,65	38,64	12,89	12,89
G3	4Apr18-3B	10,94	42,96	25,22	12,46	8,42
G2	6Apr18-3B	41,59	41,63	7,4	4,94	4,45
G2	6Apr18-3B	25,46	29,52	3,06	20,07	21,89
G4	6Apr18-3B	10,62	10,48	72,24	4,22	2,44
G1	6Apr18-3B	38,19	52,95	0,00	4,90	3,97

Based on the percentage of end members in garnet grains, they were classified into four groups (see Figure 33). G1, garnets with 0% of spessartine and high pyrope and almandine content; G2, garnets with less than 10% of spessartine and high pyrope and almandine content; G3, garnets with 24-39% of spessartine, variable amount of almandine (ranging from 26,65% to 59,9%); and G4: garnets with more than 70% of spessartine and with almost the same almandine and pyrope content. Generally, the amount of Ca-bearing end members (grossular, and andradite) is low (less than 6%) except for two samples of G3 that have close to 13% and one sample of G2 that has close to 22% of each Ca-bearing end-member.

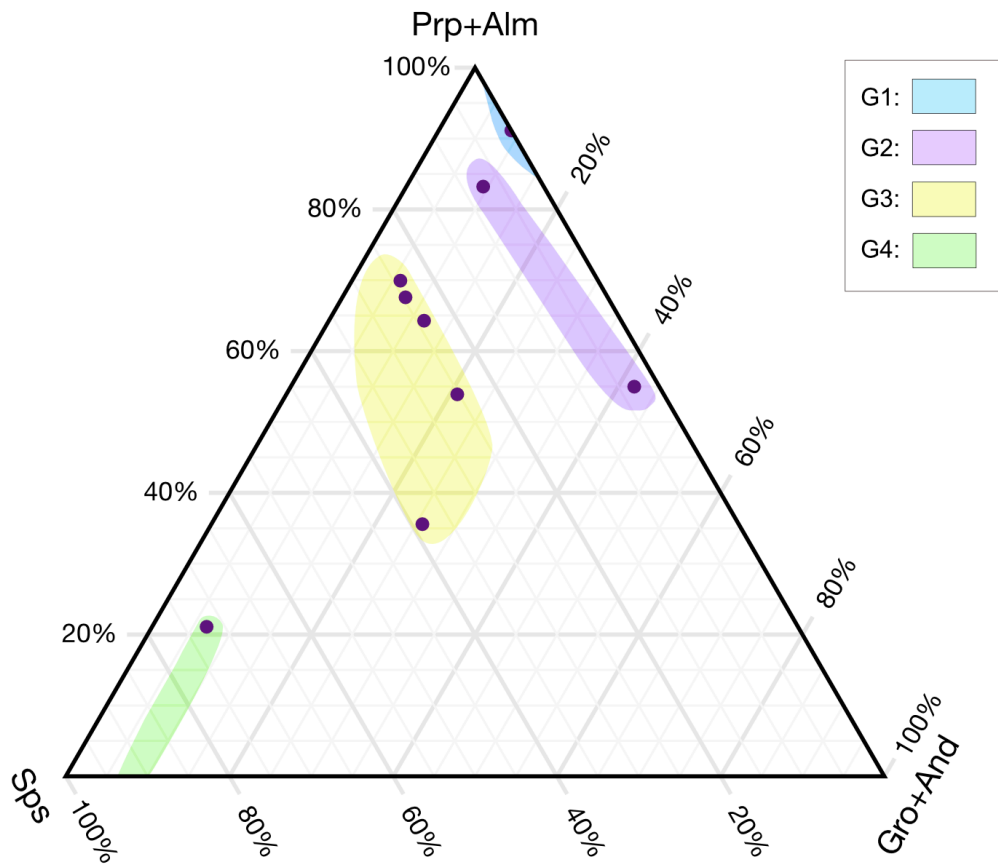


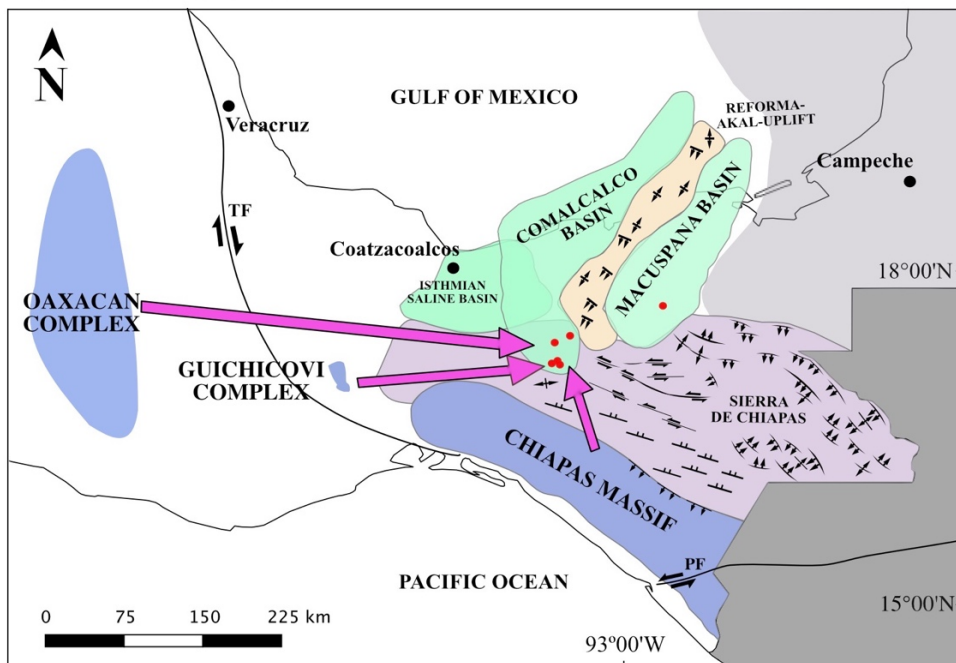
Figure 33. Ternary diagram for garnet. Legend: Prp: pyrope, Alm: almandine, Sps: spessartine, Gro: Grossular, And: Andradite. Analyzed garnets are divided into four groups by convenience according to their chemical composition: G1, G2, G3, and G4.

6. DISCUSSION

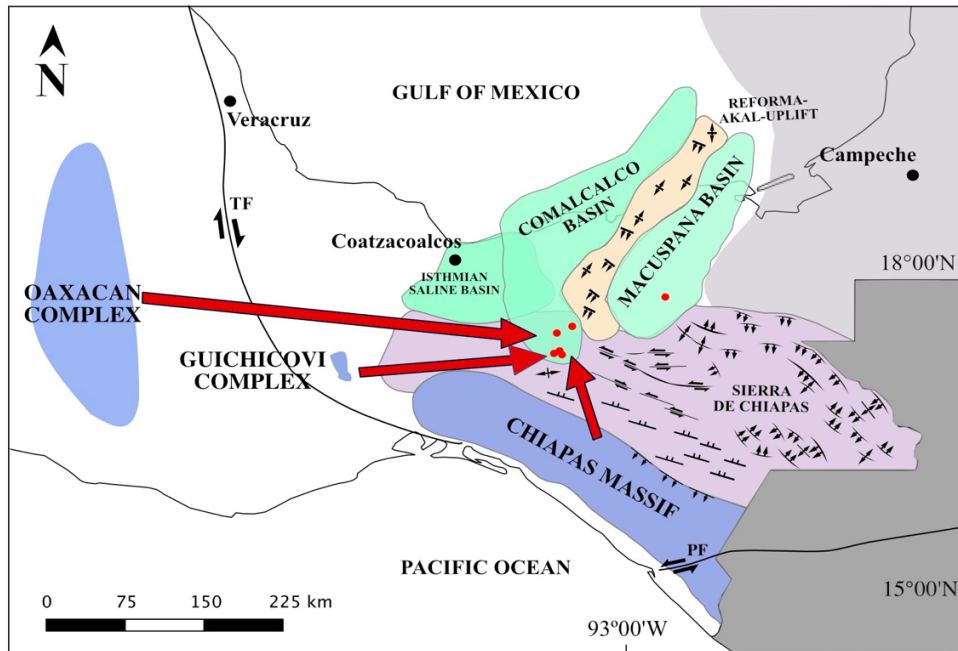
Heavy mineral suites

Several heavy mineral grains were found in the samples as Ti-bearing amphibole, apatite, chlorite, chloritoid, chromian spinel, epidote, garnet, ilmenite, rutile, staurolite, titanite, and zircon. There was not found a clear pattern for the distribution of all heavy minerals toward the basins (see Figure 13); however it was possible to recognize a pattern for some of them (see Figure 34): 1) Apatite and Staurolite are abundant in lower Miocene sediments, 2) Chloritoid is abundant in the middle Miocene sediments, 3) Rutile can be widespread distributed, but abundant in the middle Miocene sediments, 4) Ilmenite the more abundant in the middle to upper Miocene sediments, 5) Epidote only found in the upper Miocene sediments, and 6) garnet seems to be present mostly into the shallower formations from middle to upper Miocene sediments.

LOWER MIOCENE



MIDDLE MIOCENE



MIDDLE TO UPPER MIOCENE

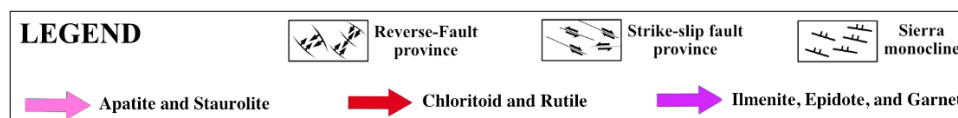
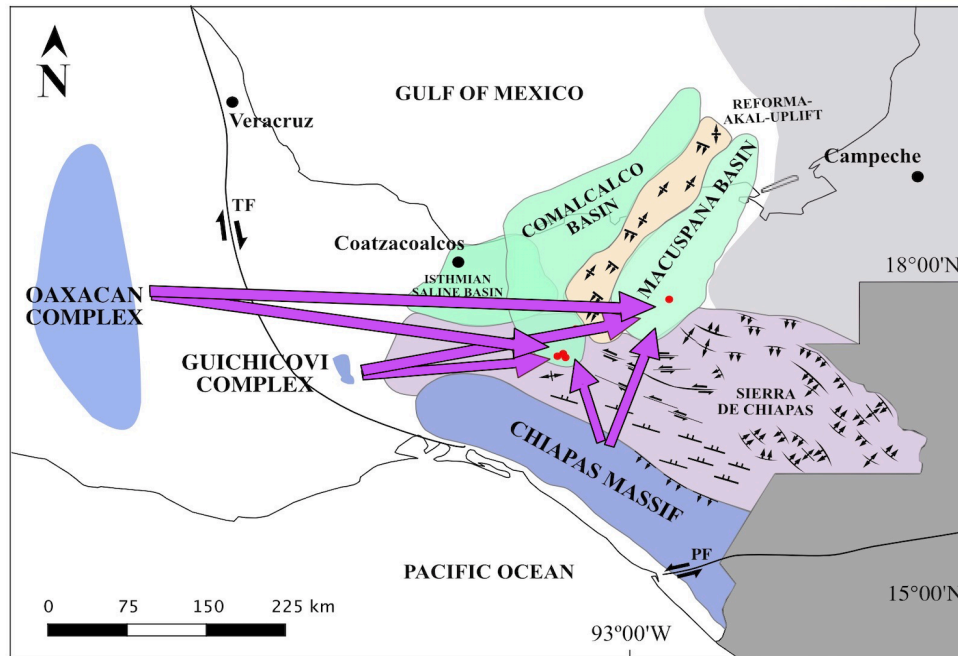


Figure 34. Pattern for the distribution of some heavy minerals toward the basins during Miocene: Apatite and Staurolite in the lower Miocene, Chloritoid and Rutile in the middle Miocene, and Ilmenite, Epidote, and Garnet in the middle to upper Miocene.

Ti-bearing amphiboles are present in the Amate Formation of the Macuspana basin, and Nanchital Shale, Filisola, and Depósito Formations of the Comalcalco basin, reaching almost 70% of the heavy mineral suite in the sample from the Depósito Formation. These amphibole, rich in Ti, could originate from the felsic orthogneisses from the Guichicovi Complex. According to Weber & Hecht (2003), amphibole is the most abundant mafic mineral in the orthogneisses of the Guichicovi Complex.

Apatite grains were found in the Amate Formation of the Macuspana basin, and the Nanchital Shale and Filisola Formations of the Comalcalco basin, ranging from 2 to 21% of the heavy mineral suite. Widespread occurrence of apatite in igneous systems (felsic, mafic, ultramafic; Piccoli & Candela, 2002) advocate the provenance of apatite grains from the three complexes of Chiapas Massif Complex, Grenvillian Oaxacan Complex, and Guichicovi Complex.

Chlorite was found in Encanto Formation and in the Nanchital Shale of the Comalcalco basin, ranging from 1 to almost 12% of the heavy mineral suite. Because it may be formed authigenically in the basins, it cannot be a reliable proxy mineral for provenance.

Chloritoid was found in the Encanto Formation of the Comalcalco basin, representing 30% of the heavy mineral suite. According to Deer et al. (1992), this is a common mineral in low- to medium-grade metapelites; thus, this had could come from the metapelite rocks of Chiapas Massif Complex (Weber et al., 2007) or the pelitic gneisses of the Oaxacan Complex (Ortega-Gutierrez, 1981).

Chromian spinel was found in Amate Formation of the Macuspana basin, and Depósito Formation and Nanchital Shale of the Comalcalco basin, ranging from 8 to 32% of the heavy mineral suite. This is the most abundant heavy mineral in the sample from Nanchital Shale. According to Roeder & Poustovetov (2001), this mineral is commonly found in MOR basaltic lavas. Chromian spinel could be derived from the amphibolites of the Chiapas Massif Complex, which have E-MORB composition (Weber et al., 2018).

Considerable amount of *Epidote* (about 20% of the heavy mineral suite) found in Amate Formation of Macuspana basin. This mineral was likely derived from amphibolite and greenschist facies from the metamorphic rocks of the Oaxacan Complex (Keppie et al., 2001),

of the amphibolites of Guichicovi Complex (Weber & Hecht, 2003), since epidote is common in rocks of greenschist and epidote-amphibolite facies (Deer et al., 1982).

Garnet was found in the Amate Formation of the Macuspana basin, and in the Nanchital Shale, Filisola, and Encanto Formations of the Comalcalco basin, ranging from 4 to 34% of the heavy mineral suite. Sample No. 2Apr18-5B from the Encanto Formation contains the highest amount of garnet. Garnet could originate from garnet amphibole gneisses from Chiapas Massif Complex. Furthermore, garnet could be sourced by the granitic garnetiferous rocks (G4) and the pelitic gneisses rich in garnet from the Grenvillian Oaxacan Complex (Ortega-Gutierrez, 1981). Also, the metasedimentary sequences composed of feldspathic gneisses (G3; Weber & Hecht, 2003), the granulites of mafic composition in which garnet is the major phase (G1; Weber & Hecht, 2003), and the garnet-bearing quartz-feldspathic gneisses (Weber & Hecht, 2003) - all from the Guichicovi Complex - could be the source of garnet to the basins.

Ilmenite was found in the Amate Formation of the Macuspana basin, and in the Filisola, Encanto, and Depósito Formations of the Comalcalco basin, ranging from 10 to 41% of the heavy minerals suite. This is the most abundant heavy mineral in the sample from the Filisola Formation (41%). The high amount of ilmenite in all samples could be derived from the rutile-bearing ilmenitites located at the southern part of the Chiapas Massif Complex (Weber et al., 2018), as well as the ilmenite-magnetite-apatite and apatite-ilmenite-rich gneisses from the Grenvillian Oaxacan Complex (Ortega-Gutierrez, 1981). Moreover, this mineral could have been sourced from the granulites of mafic composition of the Guichicovi Complex, which contains high amount of ilmenite (Weber & Hecht, 2003).

Rutile was found in the Amate Formation of the Macuspana basin, and in the Encanto Formation and Nanchital Shale of the Comalcalco basin, ranging from 1 to 22% of the heavy mineral suite. We discarded the option that they formed authigenically in the basins because if rutile form as an authigenic mineral, it shows a needle or thin lath shapes (Mange & Maurer, 1992), which was not observed in the studied samples. Rutile form predominantly in metamorphic conditions (Luvizotto & Zack 2009), thus rutile grains could be sourced from the three surrounding metamorphic complexes: Chiapas Massif, Grenvillian Oaxacan, and Guichicovi.

Staurolite was found only in the Nanchital Shale of the Comalcalco basin, being the 6% of the heavy mineral suite. Staurolite form mainly in metamorphic conditions (Mange & Maurer,

2012); as the same case of rutile, staurolite grains could be derived from any of the three surrounding metamorphic complexes: Chiapas Massif, Grenvillian Oaxacan, and Guichicovi.

It was found a small amount of *Titanite* in the Encanto and Depósito Formations of the Comalcalco basins, being less than 2% of the heavy mineral suite. Titanite of the Encanto Formation could be sourced by the anorthositic-tonalitic gneisses as well by the granulites of mafic composition in which titanite occurs as a secondary phase, both from the Guichicovi Complex (Weber & Hecht, 2003). Titanite of Depósito Formation (analyzed by SEM-EDS) displays low amount of Al which suggests that is not sourced from a metamorphic origin. In addition, its low amount of iron does not support that it is driven from acidic and intermediate igneous rocks. Its composition is closest to the theoretical CaTiSiO_5 composition; thus, titanite of Depósito Formation more likely originated from basic and/or ultrabasic igneous rocks (Asiedu, 2000) such as the granitoids of gabbroic composition of the Chiapas Massif Complex (Schaaf et al., 2002; Weber et al., 2007) and/or the ultrabasic orthogneiss of the Oaxacan Complex (Ortega-Gutierrez, 1981).

Finally, high abundance of *Zircon* was found in the Amate Formation of the Macuspana basin, and in the Nanchital Shale, Encanto, and Depósito Formations of the Comalcalco basin, ranging from 5 to 22% of the heavy mineral suite. Zircon is abundant in silicic and intermediate igneous rocks (Mange & Maurer, 1992), and could had been sourced by the deformed granitoids (granite to minor gabbro in composition) that are dominantly common in the Chiapas Massif Complex (Schaaf et al., 2002; Weber et al., 2007). Also, they could had been derived from the Grenvillian Oaxacan Complex, where there is abundant zircon within the host rocks (Keppie et al., 2001). Furthermore, they could have been sourced from the quartz-feldspathic gneisses, that according to Weber & Hecht (2003) are present in the Guichicovi Complex.

To summarize, for the heavy minerals found in our samples there are three possible sources, the three metamorphic complexes: Chiapas Massif, Grenvillian Oaxacan, and Guichicovi complexes. The rocks from which these minerals most probably were sourced are: 1) the deformed granitoids of granite to minor gabbro composition (Schaaf et al., 2002; Weber et al., 2007), metapelite rocks (Weber et al., 2007), rutile-bearing ilmenitites and amphibolites of E-MORB composition (Weber et al., 2018) of the Chiapas Massif Complex. 2) From the Grenvillian Oaxacan Complex the sources are orthogneisses of ultrabasic to ultrafelsic

composition, pelitic gneisses, granitic garnetiferous rocks, ilmenite-magnetite-apatite and apatite-ilmenite-rich gneisses (Ortega-Gutiérrez, 1981), amphibolite and greenschist facies metamorphic rocks (Keppie et al., 2001). 3) Related to the Guichicovi Complex, the sources are felsic orthogneisses, anorthositic-tonalitic gneisses, metasedimentary sequences composed of feldspathic gneisses, granulites of mafic composition, and garnet-bearing quartzo-feldspathic gneisses (Weber & Hecht, 2003).

Ti-bearing amphiboles is the only heavy mineral having a one origin, which related to the felsic orthogneisses from the Guichicovi Complex (Weber & Hecht, 2003). In addition, *chromian spinel* from E-MORB amphibolites of the Chiapas Massif Complex (Weber et al., 2018) is derived from one source. As these minerals show different source but were found into our samples, Comalcalco and Macuspana basins were certainly sourced by those two complexes.

Garnet chemistry

Garnet was found in four (Amate, Filisola, Encanto, Nanchital Shale) Formations. Garnet grains were classified into four groups (G1, G2, G3, and G4) based on their chemical composition (see section of garnet chemistry results). For all groups, we can discard the option of peridotites and associated eclogites as a provenance source of these two basins because according to Coleman et al. (1965) and Deer et al. (1992), those garnets contain more than 50% of pyrope end-member in composition. However, the garnet grains studied in this research have pyrope content, ranging from 9 to 42%, so peridotites and associated eclogites source is not supported. Furthermore, most garnet grains have a low amount of Ca-bearing end members (garnets that belong to sample No. 2Apr18-5B of Encanto Formation, 66% of grains of sample No. 3Apr18-1A of the Filisola Formation, and 75% of grains of sample No. 6Apr18-3B of the Amate formation). According to Morton (1985b) garnets with low-Ca are more stable than high-Ca garnets. Thus, it is probable that high-Ca garnets did not resist the mechanical and diagenesis processes and were not preserved into the basins. However, we should take into account that epidote that is even less stable than garnet was found in the Amate Formation.

Based on the chemical composition, each garnet group was attributed to the host rock where they occur. So, the G1 group, which is defined by none spessartine, low-grossular and high pyrope-

almandine garnets, is only formed in high-grade (granulite facies) metasediments or charnockites (Hallsworth & Chisholm, 2008). It was not attributed a specific host rock for garnets of the G2 group as containing low- spessartine, high-pyropo-almandine content, and variable amount of grossular and andradite. The G3 garnet group, which has medium-high-spessartine and pyropo content, the source could be intermediate to acidic gneisses because garnets are generally Fe-rich, Mg-low, and have variable Mn and Ca amounts (Morton et al., 2004). The G4 group of garnets, which have high spessartine content and almost the same amount of almandine than pyropo content, could have as source granites and/or granitic pegmatites because $Mn_3Al_2Si_3O_{12}$ -rich garnets are commonly found in these rocks, often as spessartine–almandine. Spessartine also occurs in Mn-rich assemblages of metasomatic origin, and in Mn-rich cherts in blueschist facies rocks (Suggate & Hall, 2014).

7. CONCLUSIONS

- The heavy minerals found in the Miocene sediments of Comalcalco and Macuspana basins of Southeast of Mexico, are twelve minerals, including Ti-bearing amphibole, apatite, chlorite, chloritoid, chromian spinel, epidote, garnet, ilmenite, rutile, staurolite, titanite, and zircon. The most common ones are Ti-bearing amphibole, chromium spinel, garnet, ilmenite, rutile, and zircon. Among the common mentioned heavy minerals, Ti-bearing amphibole, chromium spinel, garnet, and ilmenite occur higher than 30 % modal abundance.
- Some of the found heavy mineral grains analyzed in the samples show a temporal pattern of deposition in the stratigraphic section: 1) Apatite and Staurolite are abundant in lower Miocene sediments, 2) Chloritoid and Rutile are abundant in the middle Miocene sediments, 3) Ilmenite is the more abundant heavy mineral in the middle to upper Miocene sediments, 4) Epidote is only found in the upper Miocene sediments, and 6) garnet is mostly present into the shallower formations from middle to upper Miocene.
- The unique heavy minerals that suggest just one source area from which they were derived are the Ti-bearing amphibole and the chromian spinel, originated from the felsic orthogneisses of the Guichicovi Complex and the E-MORB amphibolites of the Chiapas Massif Complex respectively. Thus, Comalcalco and Macuspana basins were certainly sourced by those two complexes.
- Based on chemical composition of garnets, they were classified into four groups. G1 with none spessartine, low-grossular and high pyrope-almandine garnets, G2 with low-spessartine and high-pyrope-almandine content garnets, G3 with medium-high-spessartine and pyrope content garnets, and G4 with high spessartine content and almost the same amount of almandine than pyrope content garnets. This probably suggest different source areas for each group.
- Based on the SEM-EDS results of the heavy mineral suites studied here, we suggest that they are originated from the Chiapas Massif, Grenvillian Oaxacan, and Guichicovi complexes, which agree with previous studies.

- From literature, we know that Chiapas Massif Complex has a high amount of granitoids including those of granite composition. They will source with a high content of quartz toward the basins, being quartz essential to originate a high permeable rock and become a reservoir. The Chromian spinel found in the Amate Formation from the Macuspana basin, and the Encanto Formation and Nanchital Shale from Comalcalco basin, derived from Chiapas Massif Complex shows a high probability for those stratigraphic Units to be good oil reservoirs.

8. REFERENCES

- Ambrose, W. A., Jones, R.H., Fouad, K., Wawrzyniec, T.F., Jennette, D.C, Sakurai, S., Guevara, E. H.; Meneses-Rocha, J., Lugo, J., Aguilera, L., Berlanga, J., Miranda, L., Ruiz Morales, J., Rojas, R. (2004). Sandstone and Architecture of Miocene Upper Pliocene Shoreface, Deltaic, and Valley-fill Complexes, Macuspana Basin, Southeastern Mexico. *The University of Texas at Austin, Bureau of Economic Geology Report of Investigations No. 270.*
- Ambrose, W.A., Wawrzyniec, T.F., Fouad, K., Talukdar, S.C., Jones, R.H., Jennette, D.C., Holtz, M.H., Sakurai, S., Dutton, S.P., Dunlap, D.B., Guevara, E.H., Meneses-Rocha, J., Lugo J., Aguilera, L., Berlanga, J., Miranda, L., Ruiz, J., Rojas, R., Solís, H. (2003). Geologic framework of upper Miocene and Pliocene gas plays of the Macuspana Basin, Southeastern Mexico. *American Association of Petroleum Geologists Bulletin*, 87(9), 1411-1435.
- Ángeles-Aquino, F. J., Reyes-Núñez, J., & Quezada-Muñetón, J. M. (1992). Evolución tectónica de la Sonda de Campeche, estilos estructurales resultantes y su implicación en la generación y acumulación de hidrocarburos: *II Simposio de Exploración Petrolera. Instituto Mexicano del Petróleo, México, DF.*
- Arai, S., & Okada, H. (1991). Petrology of serpentine sandstone as a key to tectonic development of serpentine belts. *Tectonophysics*, 195(1), 65-81.
- Argyelán, G. B. (1996). Geochemical investigations of detrital chrome spinels as a tool to detect an ophiolitic source area (Gerecse Mountains, Hungary). *Acta Geologica Hungarica*, 39(4), 341-68.
- Asiedu, D. K., Suzuki, S., & Shibata, T. (2000). Provenance of sandstones from the Lower Cretaceous Sasayama Group, inner zone of southwest Japan. *Sedimentary Geology*, 131(1-2), 9-24.
- Ballard, M. M., Van der Voo, R., & Urrutia-Fucugauchi, J. (1989). Paleomagnetic results from Grenvillian-aged rocks from Oaxaca, Mexico: evidence for a displaced terrane. *Precambrian Research*, 42(3-4), 343-352.
- Bernstein, S., Frei, D., McLimans, R. K., Knudsen, C., & Vasudev, V. N. (2008). Application of CCSEM to heavy mineral deposits: Source of high-Ti ilmenite sand

- deposits of South Kerala beaches, SW India. *Journal of Geochemical Exploration*, 96(1), 25-42.
- Blatt, H. (1967). Provenance determinations and recycling of sediments. *J. Sedim. Petrol.* 37, 1031-44.
 - Bluck, B. J. (1976). 18.—Sedimentation in some Scottish rivers of low sinuosity. *Earth and Environmental Science Transactions of the Royal Society of Edinburgh*, 69(18), 425-456.
 - Brady, J. and Perkins, D. (2017). *Mineral Formulae Recalculation*. [online] Teaching Phase Equilibria. Available at: https://serc.carleton.edu/research_education/equilibria/mineralformulaerecalculation.html?fbclid=IwAR1H3pvQFZdcOb7Wo3kK5D1_pKzljBt2UIBk8pt9N-59XKL7ZKA_5wOB1OQ [Accessed 8 Dec. 2019].
 - Brichau, S., Witt, C., & Carter, A. (2008). Thermochronology applied to the Chiapas mountains, Mexico. In *AGU Fall Meeting Abstracts*.
 - Carfantan, J. C. (1985). Du système cordillerain nord-américain au domaine caraïbe étude géologique du Mexique méridional. *Université de Savoie*. Doctoral dissertation
 - Chavez, M. C., Clara, M. D. L., Juárez, J. I., Alor, I., Mata, M., Villagrán, R., Guerrero, M., Ghosh Santosh (2009). A new multidisciplinary focus in the study of the Tertiary plays in the Sureste Basin, Mexico. In: *C. Bartolini and J. R. Román Ramos (Eds.). AAPG Memoir 90. Petroleum systems in the southern Gulf of Mexico*, 155-190.
 - Chopin, C. (1983). Magnesiochloritoid and magnesiochloritoid; Two index minerals of pelitic blueschists and their preliminary phase relations in the model system MgO-Al₂O₃-SiO₂-H₂O. *American Journal of Science*, 283, 72-96.
 - Cipriani, N. (1996). Minéraux of Roches: Recherche, Classification, Utilisation. *Librairie Gründ*, 167 p., Paris.
 - Coleman, R. G., Lee, D. E., Beatty, L. B., & Brannock, W. W. (1965). Eclogites and eclogites: their differences and similarities. *Geological Society of America Bulletin*, 76(5), 483-508.
 - Cookenboo, H. O., Bustin, R. M., & Wilks, K. R. (1997). Detrital chromian spinel compositions used to reconstruct the tectonic setting of provenance: implications for orogeny in the Canadian Cordillera. *Journal of Sedimentary Research*, 67(1), 116-123.

- Damon, P. E., Shafiqullah, M., & Clark, K. F. (1981). Evolución de los arcos magmáticos en México y su relación con la metalogénesis. *Revista Mexicana de Ciencias Geológicas*, 5(2), 223-238.
- Deer, W. A., Howie, R. A., & Zussman, J. (1982). Rock-forming minerals: Orthosilicates, Volume 1A. *Geological Society of London*, London.
- Dewey, J. F., & Burke, K. C. (1973). Tibetan, Variscan, and Precambrian basement reactivation: products of continental collision. *The Journal of Geology*, 81(6), 683-692.
- Dick, H. J., & Bullen, T. (1984). Chromian spinel as a petrogenetic indicator in abyssal and alpine-type peridotites and spatially associated lavas. *Contributions to Mineralogy and Petrology*, 86(1), 54-76.
- Dickinson, W. R., & Lawton, T. F. (2001). Carboniferous to Cretaceous assembly and fragmentation of Mexico. *Geological Society of America Bulletin*, 113(9), 1142-1160.
- Duarte, E., Cardona, A., Lopera, S., Valencia, V., & Estupiñan, H. (2018). Provenance and diagenesis from two stratigraphic sections of the lower cretaceous Caballos Formation in the upper Magdalena Valley: geological and reservoir quality implications. *CT&F-Ciencia, Tecnología y Futuro*, 8(1), 5-29.
- Estrada-Carmona, J., Weber, B., Martens, U., & López-Martínez, M. (2012). Petrogenesis of Ordovician magmatic rocks in the southern Chiapas Massif Complex: relations with the early Palaeozoic magmatic belts of northwestern Gondwana. *International Geology Review*, 54(16), 1918-1943.
- Faupl, P., Pavlopoulos, A., Klotzli, U., & Petrakakis, K. (2006). On the provenance of mid-Cretaceous turbidites of the Pindos zone (Greece): implications from heavy mineral distribution, detrital zircon ages and chrome spinel chemistry. *Geological Magazine*, 143(3), 329-342.
- Fleet, W. F. (1926). Petrological notes on the Old Red Sandstone of the West Midlands. *Geological Magazine*, 63(11), 505-516.
- Fries, C., Schlaepfer, C. J., & Orta, C. R. (1966). Nuevos datos geocronológicos del Complejo Oaxaqueño. *Boletín de la Sociedad Geológica Mexicana*, 29(1), 59-66.
- Garzanti, E. (2016). From static to dynamic provenance analysis—Sedimentary petrology upgraded. *Sedimentary Geology*, 336, 3-13.

- González-Lara, J.C. (2001) Le Paléocène du Chiapas (SE du Mexique): Biostratigraphie, Sédimentologie et Stratigraphie Séquentielle. *Géologie Alpine*, Mémoire H.S. No 36, 139 p., Grenoble.
- Guzmán-Speziale, M., & Meneses-Rocha, J. J. (2000). *The North America–Caribbean plate boundary west of the Motagua–Polochic fault system: a fault jog in Southeastern Mexico*. *Journal of South American Earth Sciences*, 13(4-5), 459–468.
- Hallsworth, C. R., & Chisholm, J. I. (2008). Provenance of late Carboniferous sandstones in the Pennine Basin (UK) from combined heavy mineral, garnet geochemistry and palaeocurrent studies. *Sedimentary Geology*, 203(3-4), 196-212.
- HAO, Q., LI, L., ZUO, Y., CHEN, W., WU, L., & YI, J. (2018). *Petroleum Distribution Characteristics of the Americas and the Exploration Prospect Analysis*. *Acta Geologica Sinica - English Edition*, 92(1), 378–393.
- Haughton, P. D. W., S. P. Todd, and A. C. Morton. (1991). Sedimentary provenance studies. In A. C. Morton, S. P. Todd, & P. D. W. Haughton (Eds.), *Developments in Sedimentary Provenance Studies* (pp. 1-11). Geological Society Special Publication No. 57. London.
- Hisada, K., & Arai, S. (1993). Detrital chrome spinels in the Cretaceous Sanchu sandstone, central Japan: indicator of serpentinite protrusion into a fore-arc region. *Palaeogeography, Palaeoclimatology, Palaeoecology*, 105(1-2), 95-109.
- Howie, R. A., Zussman, J., & Deer, W. (1992). *An introduction to rock-forming minerals*. Longman.
- Hubert, J. F. (1962). A zircon-tourmaline-rutile maturity index and the interdependence of the composition of heavy mineral assemblages with the gross composition and texture of sandstones. *Journal of Sedimentary Research*, 32(3), 440-450.
- Hubert, J. F. (1971). Analysis of heavy mineral assemblages. *Procedures in sedimentary Petrology*, In R. E. Carver. (Ed.), 453-78. Wiley. New York.
- John W. A., Bideaux, B. A., Bladh, K. W., and Nichols, M. C. (Eds.) (2001). *Handbook of Mineralogy*, Mineralogical Society of America. USA, <http://www.handbookofmineralogy.org/>.
- Keppie, J. D., Dostal, J., Ortega-Gutiérrez, F., & López, R. (2001). A Grenvillian arc on the margin of Amazonia: evidence from the southern Oaxacan Complex, southern Mexico. *Precambrian Research*, 112(3-4), 165-181.

- Kesler, S. E., & Heath, S. A. (1970). Structural trends in the southernmost North American Precambrian, Oaxaca, Mexico. *Geological Society of America Bulletin*, 81(8), 2471-2476.
- Kesler, S. E. (1973). Basement rock structural trends in southern Mexico. *Geological Society of America Bulletin*, 84(3), 1059-1064.
- Lee, Y. I. (1999). Geotectonic significance of detrital chromian spinel: a review. *Geosciences Journal*, 3(1), 23.
- Lenaz, D., Kamenetsky, V. S., Crawford, A. J., & Princivalle, F. (2000). Melt inclusions in detrital spinel from the SE Alps (Italy–Slovenia): a new approach to provenance studies of sedimentary basins. *Contributions to Mineralogy and Petrology*, 139(6), 748-758.
- Lenaz, D., Kamenetsky, V. S., & Princivalle, F. (2003). Cr-spinel supply in the Brkini, Istrian and Krk Island flysch basins (Slovenia, Italy and Croatia). *Geological Magazine*, 140(3), 335-342.
- Luvizotto, G. L., & Zack, T. (2009). Nb and Zr behavior in rutile during high-grade metamorphism and retrogression: an example from the Ivrea–Verbano Zone. *Chemical Geology*, 261(3-4), 303-317.
- Mackie, W. (1923). The principles that regulate the distribution of particles of heavy minerals in sedimentary rocks, as illustrated by the sandstones of north-east Scotland. *Transactions of the Edinburgh Geological Society*, 11(2), 138-164.
- Mange, M. A., & Maurer, H. F. (1992). Heavy minerals in colour. *Chapman and Hall*. London.
- Mange, M. A., & Wright, D. T. (Eds.). (2007). Heavy minerals in use (Vol. 58). *Developments in sedimentology*, Vol. 58, *Elsevier*.
- Meneses-Rocha, J. J. (2001). Tectonic evolution of the Ixtapa graben, an example of a strike-slip basin in southeastern Mexico: Implications for regional petroleum systems. In C. Bartolini, R. T. Buffler, and A. CantúChapa. (Eds.), *The western Gulf of Mexico Basin: Tectonics, sedimentary basins, and petroleum systems* (183-216); AAPG Memoir 75.
- Mora, C. I. (1983). The temperature/pressure conditions of Grenville-age granulite-facies metamorphism of the Oaxacan Complex, Southern Mexico. Rice University. Doctoral dissertation, Houston.

- Mora, C. I., & Valley, J. W. (1985). Ternary feldspar thermometry in granulites from the Oaxacan Complex, Mexico. *Contributions to Mineralogy and Petrology*, 89(2-3), 215-225.
- Morton, A. C. (1985a). Heavy minerals in provenance studies. In: *Provenance of Arenites*, pp. 249-277, Dordrecht. Springer.
- Morton, A. C. (1985b). A new approach to provenance studies: electron microprobe analysis of detrital garnets from Middle Jurassic sandstones of the northern North Sea. *Sedimentology*, 32(4), 553-566.
- Morton, A. C. (1991). Geochemical studies of detrital heavy minerals and their application to provenance research. In: *A. C. Morton, S. P. Todd, & P. D. W. Haughton (Eds.), Developments in Sedimentary Provenance Studies* (pp. 31-45). Geological Society Special Publication No. 57. London.
- Morton, A. C., & Hallsworth, C. (1994). Identifying provenance-specific features of detrital heavy mineral assemblages in sandstones. *Sedimentary Geology*, 90(3-4), 241-256.
- Morton, A., Hallsworth, C., & Chalton, B. (2004). Garnet compositions in Scottish and Norwegian basement terrains: a framework for interpretation of North Sea sandstone provenance. *Marine and Petroleum Geology*, 21(3), 393-410.
- Murillo-Muñetón, G., Anderson, J. L., & Tosdal, R. M. (1994). A new Grenville-age granulite terrane in southern Mexico. *Geol. Soc. Am. Abs. Programs*, 26(2), 76.
- Murillo-Muñetón, G. (1996). Petrologic and geochronologic study of Grenville-age granulites and post-granulite plutons from the La Mixtequita area, state of Oaxaca in southern Mexico, and their tectonic significance. University of Southern California.
- Narváez-Rodríguez, J. Y., Helenes-Escamilla, J., del Moral-Domínguez, J. M., Martínez-Morales, V. M., Macías-Ojeda, C., Castillejos-Zurita, O. G., & Sánchez-Ríos, M. A. (2008). Bioestratigrafía de secuencias del Mioceno-Plioceno de la cuenca Macuspana, sureste del Golfo de México. *Revista Mexicana de Ciencias Geológicas*, 25(2), 217-224.
- Nieto-Samaniego, A. F., Alaniz-Álvarez, S. A., Silva-Romo, G., Eguiza-Castro, M. H., & Mendoza-Rosales, C. C. (2006). Latest Cretaceous to Miocene deformation events in the eastern Sierra Madre del Sur, Mexico, inferred from the geometry and age of major structures. *Geological Society of America Bulletin*, 118(1-2), 238–252.

- Odom, I. E., Doe, T. W., & Dott, R. H. (1976). Nature of feldspar-grain size relations in some quartz-rich sandstones. *Journal of Sedimentary Research*, 46(4), 862-870.
- Ortega-Gutiérrez, F. (1981). Metamorphic belts of southern Mexico and their tectonic significance. *Geofísica Internacional*, 20(3).
- Ortega-Gutiérrez, F. (1984). Evidence of Precambrian evaporites in the Oaxacan granulite complex of southern Mexico. *Precambrian Research*, 23(3-4), 377-393.
- Ortega-Gutiérrez, F., Ruiz, J., & Centeno-García, E. (1995). Oaxaquia, a Proterozoic microcontinent accreted to North America during the late Paleozoic. *Geology*, 23(12), 1127-1130.
- Owens, B. E., & Dymek, R. F. (1992). Fe-Ti-P-rich rocks and massif anorthosites: problems of interpretation illustrated from the Labrieville and St-Urbain plutons, Quebec. *The Canadian Mineralogist*, 30(1), 163-190.
- Owens, B. E., Rockow, M. W., & Dymek, R. F. (1993). Jotunites from the Grenville Province, Quebec: Petrological characteristics and implications for massif anorthosite petrogenesis. *Lithos*, 30(1), 57-80.
- Padilla y Sánchez, R. J. (2007). Evolución geológica del sureste mexicano desde el Mesozoico al presente en el contexto regional del Golfo de México. *Boletín de la Sociedad Geológica Mexicana*, 59(1), 19-42.
- Peterson, J. A. (1983). Petroleum geology and resources of southeastern Mexico, northern Guatemala, and Belize (p. 44). *United States Department of the Interior, Geological Survey Circular 760*.
- Pettijohn, F. J., Potter, P. E., & Siever, R. (1973). Sand and Sandstone. *Springer Verlag*. New York.
- Pettijohn, F. J., Potter, P. E., & Siever, R. (1987). Sandy depositional systems. In: *Sand and Sandstone* (pp. 341-423). Springer, New York.
- Piccoli, P. M., & Candela, P. A. (2002). Apatite in Igneous Systems. *Reviews in Mineralogy and Geochemistry*, 48(1), 255-292.
- Pindell, J., & Miranda, E. (2011). Linked Kinematic Histories of the Macuspana, Akal-Reforma, Comalcalco, and Deepwater Campeche Basin Tectonic Elements, Southern Gulf of Mexico. *Transactions- Gulf Coast Association of Geological Societies*, 61, 353-362.

- Planckaert, M. (2005). Oil reservoirs and oil production. In: *Petroleum microbiology* (pp. 3-19). American Society of Microbiology.
- Pober, E., & Faupl, P. (1988). The chemistry of detrital chromian spinels and its implications for the geodynamic evolution of the Eastern Alps. *Geologische Rundschau*, 77(3), 641-670.
- Press, S. (1986). Detrital spinels from alpinotype source rocks in Middle Devonian sediments of the Rhenish Massif. *Geologische Rundschau*, 75(2), 333-340.
- Reed, S. J. B. (2005). Electron microprobe analysis and scanning electron microscopy in geology. *Cambridge University Press*, London.
- Roeder, P. L., Poustovetov, A., & Oskarsson, N. (2001). Growth forms and composition of chromian spinel in MORB magma: diffusion-controlled crystallization of chromian spinel. *The Canadian Mineralogist*, 39(2), 397–416.
- Rosales-Domínguez, M. del C., Bermúdez-Santana, J. C., & Aguilar-Piña, M. (1997). *Mid and Upper Cretaceous foraminiferal assemblages from the Sierra de Chiapas, southeastern Mexico. Cretaceous Research*, 18(5), 697–712. doi:10.1006/cres.1997.0081
- Ruiz, J., Tosdal, R. M., Restrepo, P. A., & Murillo-Muñetón, G. (1999). Pb isotope evidence for Colombia-southern Mexico connections in the Proterozoic. *Special Papers-Geological Society of America*, 183-198.
- Schaaf, G. P. E., Weber, B., Weis, P., Groß, A., Ortega-Gutiérrez, F., & Köhler, H. (2002). The Chiapas Massif (Mexico) revised: New geologic and isotopic data and basement characteristics. *Neues Jahrbuch für Geologie und Palaontologie-Abhandlungen*, 225(1), 1-23.
- Servicio Geológico Mexicano, (2008). Carta Geológica-Minera Estatal Chiapas y Tabasco, escala 1:500,000: Pachuca, Hidalgo, México. *Consejo de Recursos Minerales*, 1 map.
- Solari, L. A., López, R., Cameron, K. L., Ortega-Gutiérrez, F., & Keppie, J. D. (1998). Reconnaissance U/Pb geochronology and common Pb isotopes of the northern part of the ~ 1 Ga Oaxacan Complex, southern Mexico. In: *EOS American Geophysical Union 1998 Fall Meeting* (Vol. 79, No. 45, p. F931).
- Suggate, S. M., & Hall, R. (2014). Using detrital garnet compositions to determine provenance: a new compositional database and procedure. In A. C. Morton, N.

- Richardson, R. A. Scott, H. R. Smyth (Eds.), *Sediments Provenance Studies in Hydrocarbon Exploration and Production* (pp. 373-393). Geological Society Special Publication No. 386, London.
- Van Andel, T. H. (1959). Reflections on the interpretation of heavy mineral analyses. *Journal of Sedimentary Research*, 29(2), 153-163.
 - Van Harten, D. (1965). On the estimation of relative grain frequencies in heavy mineral slides. *Geol. Mijnb.* 44, 357-63.
 - Weber, B. (1998). *Die magmatische und metamorphe Entwicklung eines kontinentalen Krustensegments: Isotopengeochemische und geochronologische Untersuchungen am Mixtequita-Komplex, Südostmexiko*. Inst. für Allg. u. Angewandte Geologie d. Ludwig-Maximilians-Univ.
 - Weber, B., & Köhler, H. (1999). Sm–Nd, Rb–Sr and U–Pb geochronology of a Grenville Terrane in Southern Mexico: origin and geologic history of the Guichicovi Complex. *Precambrian Research*, 96(3-4), 245-262.
 - Weber, B., & Hecht, L. (2003). Petrology and geochemistry of metaigneous rocks from a Grenvillian basement fragment in the Maya block: the Guichicovi complex, Oaxaca, southern Mexico. *Precambrian Research*, 124(1), 41-67.
 - Weber, B., Iriondo, A., Premo, W. R., Hecht, L., & Schaaf, P. (2007). New insights into the history and origin of the southern Maya block, SE México: U–Pb–SHRIMP zircon geochronology from metamorphic rocks of the Chiapas massif. *International Journal of Earth Sciences*, 96(2), 253-269.
 - Weber, B., Valencia, V. A., Schaaf, P., Pompa-Mera, V., & Ruiz, J. (2008). Significance of provenance ages from the Chiapas Massif Complex (southeastern Mexico): redefining the Paleozoic basement of the Maya Block and its evolution in a peri-Gondwanan realm. *The Journal of Geology*, 116(6), 619-639.
 - Weber, B., González-Guzmán, R., Manjarrez-Juárez, R., de León, A. C., Martens, U., Solari, L., ... & Valencia, V. (2018). Late Mesoproterozoic to Early Paleozoic history of metamorphic basement from the southeastern Chiapas Massif Complex, Mexico, and implications for the evolution of NW Gondwana. *Lithos*, 300, 177-199.
 - Weissbrod, T., & Nachmias, J. (1986). Stratigraphic significance of heavy minerals in the late Precambrian-Mesozoic clastic sequence (“Nubian Sandstone”) in the Near East. *Sedimentary Geology*, 47(3-4), 263-291.

- Witt, C., Rangin, C., Andreani, L., Olaz, N., & Martinez, J. (2012). The transpressive left-lateral Sierra Madre de Chiapas and its buried front in the Tabasco plain (southern Mexico). *Journal of the Geological Society*, 169(2), 143-155.
- Worden, R. H., & Morad, S. (2000). Quartz cementation in oil field sandstones: a review of the key controversies. In: R. H. Worden & S. Morad (Eds.), *quartz cementation in oilfield sandstones*, Special Publication No. 29, International Association. Of Sedimentologists, Blackwell Science, pp. 01-20, Oxford.
- Zack, T., Kronz, A., Foley, S. F., & Rivers, T. (2002). Trace element abundances in rutiles from eclogites and associated garnet mica schists. *Chemical Geology*, 184(1-2), 97-122.
- Zhu, B., Kidd, W. S., Rowley, D. B., & Currie, B. S. (2004). Chemical compositions and tectonic significance of chrome-rich spinels in the Tianba Flysch, southern Tibet. *The Journal of Geology*, 112(4), 417-434.
- Zimmerle, W. (1984). The geotectonic significance of detrital brown spinel in sediments. *Mitt. Geol.-Paläont. Inst. Univ Hamburg*, (56), 337-360.

10. APPENDIX

APPENDIX 1

This annex contains Tables 5-10 with detailed petrographic description of minerals found in all samples. Legend: Amp: amphibole; Ap: Apatite; Chl: Chlorite; Cld: Chloritoid; Chr: Chromian spinel; Ep: Epidote; Gt: Garnet; Ilm: Ilmenite; Rt: Rutile; St: Staurolite; Ttn: Titanite; Zrn: Zircon.

Table 5. Petrographic analysis of 6Apr18-3B sample (Amate Formation, upper Miocene).

Mineral	Color	Transparency	Pleochroism	Habit	Relief	Birefringence color	Extinction angle (°)	Optic sign
Amp	Blueish green	Translucent	To green	-	Medium to High	Third order	-	-
Ap	Light yellow	Translucent	-	-	High	First order	-	-
Chr	Dark brown	Translucent	-		High	-	-	-
Ep	Light green	Translucent	Weakly		High	Third order	-	Biaxial negative
Ep	Greenish yellow	Translucent	-		High	Third order	-	-
Gt	Pink	Translucent	-		High	-	-	-
Gt	Light orange	Translucent	-		High	-	-	-
Gt	Light green	Translucent	-		High	-	-	-
Ilm	Black / Red / Brown	Opaque	-		-	-	-	-
Rt	Reddish brown	Translucent	Weakly: to dark reddish brown		High	-	-	-
Rt	Reddish orange	Translucent	Weakly		High	-	0-6	-
Zrn	-	Transparent	-		High	Fourth order	-	Uniaxial positive

Table 6. Petrographic analysis of 3Apr18-1A sample (Filisola Formation, middle-upper Miocene).

Mineral	Color	Transparency	Pleochroism	Habit	Relief	Birefringence color	Extinction angle (°)	Optic sign
Amp	Brown	Translucent	Strong to Brown	Tabular	Medium to High	Third order	-	-

Amp	Brownish green	Translucent	To dark green	Tabular	Medium	Second order	13	Biaxial negative
Ap	Brown	Translucent	Weakly to Light brown		High	First order	-	-
Ap	Gray	Translucent	To dark gray		High	First order	0 - 3	-
Gt	Dark pink	Translucent	-		High	-	-	-
Gt	Light pink	Translucent	-		High	Lower first order	-	-
Gt	-	Transparent	-		High	-	-	-
Ilm	Reddish black	opaque	-		-	-	-	-
Zrn	-	Transparent	-		High	Fourth order	-	-

Table 7. Petrographic analysis of 2Apr18-5B sample (Encanto Formation, late lower-middle Miocene).

Mineral	Color	Transparency	Pleochroic	Habit	Relief	Birefringence color	Extinction angle (°)	Optic sign
Chl	Greenish blue	Translucent	Weakly	-	Medium	First order	-	Biaxial
Chr	Black red	Opaque	-			-	-	-
Chr	Brown	Translucent	-		Medium	-	-	-
Cld	Yellow	Translucent	Greenish yellow		Medium to high	Second order	-	-
Gt	Light pink	Translucent	-		High	-	-	Uniaxial negative
Rt	Reddish brown	Translucent	Weakly		High	-	0	Uniaxial positive
Zrn	-	Transparent	-		High	Fourth order	-	-

Table 8. Petrographic analysis of 4Apr18-5A sample (Encanto Formation, late lower-middle Miocene).

Mineral	Color	Transparency	Pleochroism	Habit	Relief	Birefringence color	Extinction angle (°)	Optic sign
Chl	Light brown	Translucent	-	-	Medium	Second order	-	-
Chl	Brown	Translucent	-	-	High	-	-	-
Ilm	Black/ Red/	Opaque	-		-	-	-	-

	Brown							
Rt	Yellow	Translucent	-		High	Third order	-	-
Rt	Reddish brown	Translucent	Weakly		High	-	-	-
Ttn	Light pink	Translucent	Weakly		High	Fifth order	-	-
Zrn		Transparent	-		High	Fourth order	-	-

Table 9. Petrographic analysis of 2Apr18-2B sample (Depósito Formation, lower Miocene).

Mineral	Color	Transparency	Pleochroic	Habit	Relief	Birefringence color	Extinction angle (°)	Optic sign
Amp	Light green	Translucent	Brownish light green	-	Medium to high	Second order	0 - 5	Biaxial negative
Amp	Brown	Translucent	Dark brown green	Tabular	High	Second order	0 – 10	Biaxial negative
Ilm	Black	Opaque	-		-	-	-	-
Ttn	Yellow	Translucent	Weakly light yellow		High	Fourth order	-	-
Zrn	Light pink	Some are transparent, others are translucent	-		High	Fourth order	-	-

Table 10. Petrographic analysis of 4Apr18-3B sample (Nanchital Shale, early lower Miocene).

Mineral	Color	Transparency	Pleochroism	Habit	Relief	Birefringence color	Extinction angle (°)	Optic sign
Amp	Brown	Translucent	To grayish yellow		Medium to High	Third order	-	-
Ap	Light brown	Translucent	-		High	-	-	-
Chl	Light green	Translucent	Weakly to yellowish	Like mica	High	Second order	-	-
Chr	Reddish black	Opaque	-		-	-	-	-
Chr	Brown	Translucent	-		Medium to High	-	-	-
Gt	Light pink	Translucent			High	Lower first order	-	Uniaxial negative

Rt	Dark brown	Opaque	-		-	-	-	-
St	Gray / Bright light yellow	Translucent	To dark gray		High	Second order	-	-
Zrn	-	Transparent	-		-	-		

APPENDIX 2

This annex contains Table 11 with group of minerals and some characteristics of them.

Table 11. Group of minerals and some characteristics of them.

Specific Gravity	Mineral	Category	Formula	Crystal system	Mohs Scale
2.90	Amphibole (Ti-bearing)	Silicate	$\text{NaCa}_2(\text{Mg}_3\text{Ti}^{4+}\text{Al})(\text{Si}_6\text{Al}_2)\text{O}_{22}(\text{OH})_2$	Monoclinic	5.0-6.0
3.16-3.22	Apatite	Phosphate	$\text{Ca}_5(\text{PO}_4)_3(\text{F},\text{Cl},\text{OH})$	Hexagonal	5.0
2.64-2.74	Chlorite	Phyllosilicate	$(\text{Mg},\text{Al},\text{Fe})_{12}(\text{Si},\text{Al})_8\text{O}_{20}(\text{OH})_{16}$	Monoclinic	2.0-2.5
3.46-3.80	Chloritoid	Nesosilicate	$(\text{Fe},\text{Mg},\text{Mn})_2\text{Al}_4\text{Si}_2\text{O}_{10}(\text{OH})_4$	Monoclinic	6.5
3.58-4.4	Chromian spinel	Oxide	$(\text{Mg},\text{Fe}^{2+})(\text{Cr},\text{Al},\text{Fe}^{3+})_2\text{O}_4$	Cubic	7.5-8.0
3.30-3.60	Epidote	Sorosilicate	$\text{Ca}_2(\text{Al}_2\text{Fe}^{3+})[\text{O}(\text{OH})](\text{Si}_2\text{O}_7)(\text{SiO}_4)$	Monoclinic	6.0-7.0
	Garnet				
4.05	Almandine	Nesosilicate	$(\text{Fe}^{2+})_3\text{Al}_2(\text{SiO}_4)_3$	Cubic	7.0-7.5
3.86	Andradite	Nesosilicate	$\text{Ca}_3(\text{Fe}^{3+})_2(\text{SiO}_4)_3$	Cubic	6.5-7.0
3.61	Grossular	Nesosilicate	$\text{Ca}_3\text{Al}_2(\text{SiO}_4)_3$	Isometric	6.5-7.0
3.78	Pyrope	Nesosilicate	$\text{Mg}_3\text{Al}_2(\text{SiO}_4)_3$	Cubic	7.0-7.5
4.19	Spessartine	Nesosilicate	$(\text{Mn}^{2+})_3\text{Al}_2(\text{SiO}_4)_3$	Isometric	6.5-7.0
4.70-4.79	Ilmenite	Oxide	FeTiO_3	Trigonal	5.0-6.0
4.23	Rutile	Oxide	TiO_2	Tetragonal	6.0-6.5
3.74-3.83	Staurolite	Nesosilicate	$(\text{Fe}^{2+},\text{Mg},\text{Zn})_2\text{Al}_9(\text{Si},\text{Al})_4\text{O}_{22}\text{OH}_2$	Prismatic	7.0-7.5
3.48-3.60	Titanite	Nesosilicate	CaTiSiO_5	Tetragonal	6.0-6.5
4.6-4.7	Zircon	Nesosilicate	ZrSiO_4	Tetragonal	7.5

Source: Cipriani (1996); Mange & Maurer (1992).